Chapter 3
Mechanics of Anisotropic Composite Materials

Artur W. Ganczarski, S. Hernik and Jacek J. Skrzypek

Abstract Mechanics of composite materials was in the last decade one of the most rapidly explored engineering area, basically due to huge progress in composite fabrication and use. The main problem referred in this chapter is how to correctly predict averaged effective properties by implementation of numerous homogenization techniques. Useful classification of composites with respect to the format of effective stiffness matrix, based on the analogy between the crystal lattice symmetry and respective configuration of reinforcement in the RUC, is given. Extended section is focused on conventionally used Hill's theorem on upper and lower bounds by Voigt and Reuss' isotropic estimation for approximate determination of stiffness and compliance matrices of anisotropic composite. Consistent application of the Hill theorem to the elements of elastic stiffness or compliance matrices (but not to engineering anisotropy constants) enable to explain some peculiarities of the Poisson ratio diagrams, met in respective bibliography (e.g., Aboudi et al., Micromechanics of Composite Materials, 2013; Sun and Vaidya, Compos. Sci. Technol. 56:171–179, 1996; Gan et al., Int. J. Solids Struct. 37:5097–5122, 2000). The new effective proposal to achieve approximation of the mechanical modules of unidirectionally reinforced composites by the use of hybrid-type rule of weighted average between the Voigt and Reuss upper and lower estimates is proposed. Capability of this averaged interpolation was checked based on selected findings by Gan et al. (Int. J. Solids Struct. 37:5097–5122, 2000) for Boron/Al composite, which show good convergence and enable to treat weighting coefficients as universal ones over the full V_f range.

Keywords Symmetry of composites · Homogenization methods · Consistent use of estimates to averaged matrices · Poisson's ratio peculiarity · Anisotropic hybrid homogenization rule

A.W. Ganczarski (✉) · S. Hernik · J.J. Skrzypek
Solid Mechanics Division, Institute of Applied Mechanics,
Cracow University of Technology, al. Jana Pawła II 37, 31-864 Kraków, Poland
e-mail: Artur.Ganczarski@pk.edu.pl

S. Hernik
e-mail: hernik@mech.pk.edu.pl

J.J. Skrzypek
e-mail: Jacek.Skrzypek@pk.edu.pl

3.1 State of the Art

Essential progress observed in *manufacturing processes* and *application of composite materials* results in necessity to develop methodology of determination of the *effective properties mechanical*, *thermal*, and others. Among the variety of papers dealing with modeling of effective mechanical properties of composites and their experimental verification, the following group of papers in which a coupling between the topology of *fibrous reinforcement* (or *particle*) *reinforcement* and *material symmetry* of *constitutive model* describing composite can be distinguished, for instance: Sun and Vaidya [30], Gan et al. [9], Liu et al. [19], Würkner et al. [37], Selvadurai and Nikopour [28] and others.

Aforementioned papers deal with the modeling of *unidirectionally reinforced composites* treated as homogeneous orthotropic solids characterized by some effective modules that describe average material properties of the composite. Assuming the *periodic fiber arrangement* inside the matrix usually two types of *Representative Unit Cells* (RUC) that exhibit either the *tetragonal symmetry* (*square array*) or the *hexagonal symmetry* (*hexagonal array*) are considered.

In the significant paper by Sun and Vaidya [30] two *composite* systems: *Boron/Al* and *Graphite/Epoxy* of the respective fixed volume V_f fraction equal to 0.47 and 0.6 are analyzed. Authors find essential scatter in analytical results obtained for two kinds of composites in comparison with earlier data from the literature, namely: Hashin and Rosen [10], Whitney and Riley [35], Chamis [6], Sun and Chen [29], Sun and Zhou [31], Kenaga et al. [15]. In particular, the large scatter is referred to the effective Young modulus, the effective Kirchhoff modulus, and the effective Poisson ratio in the plane of *transverse isotropy*. The obtained material constants, in general, do not confirm the theorem on *upper* and *lower bounds* based on the classical *Voigt* and *Reuss rules*. Especially difficult is to explain the estimated magnitude of the in-plane Poisson ratio exceeding range of two composite components based on either the isotropic characteristic of components in *Boron/Al composite* or the orthotropic characteristic of components in *Graphite/Epoxy composite*.

More systematic analysis of the influence of homogenization methods on estimated effective properties of composites is due to Gan et al. [9]. The authors compare the new *Strain-Compatible Method of Cells* (SCMC) with other homogenization methods such as *Generalized Method of Cells* (GMC) Paley and Aboudi [25] and *micromechanical analysis* using FEM. For numerical simulation, authors used the unidirectionally reinforced Boron/Al composite assuming two types of the representative unit cells based either on a *random topology of* parallel *fibers* or on the hexagonal array for full spectrum of the volume fraction $V_f \in < 0, 1 >$. The homogenization results are also compared with the classical approximate calculations based on *Voigt/Reuss mixture rules*, Voigt [34], Reuss [27]. The performed analysis confirms applicability of the upper/lower bounds for majority of equivalent material constants except for the in-plane Poisson ratio. However the authors do not precisely distinguish between the tetragonal or the hexagonal symmetry when modeling

Representative Unit Cell (RUC) such that all six modules of orthotropy are treated as independent in spite of clear hexagonal symmetry in fibers topology.

Liu et al. [19] analyze possibility for the Poisson ratio positioned beyond the Voigt/Reuss estimates. Moreover: "It was found that the effective Young modulus in both transverse and longitudinal direction can exceed not only the approximate Voigt estimation, but also the stiffness of the stiffer constituent phase". The authors recommend precautions when applying Voigt/Reuss estimates in cases when one of the components is made of incompressible material.

In the recently published paper by Würkner et al. [37] the effective elastic modules of the composite formed of isotropic *Epoxy matrix* and transversely isotropic *Graphite fibers* are examined for reasonable wide range of volume fraction $V_f \in\ <0.1 \div 0.6>$ see also comments in Sect. 3.5.5 of this chapter. The rhombic array of fibers is used for simulations characterized by different topology angles of RUC. Following cases are considered: $\gamma = 60°$ (*hexagonal array*), $60° < \gamma < 90°$ (*rhombic array*) and $\gamma = 90°$ (*tetragonal array*). The estimated effective modules show satisfactory coincidence with numerical results given by Jiang et al. [14].

The more general approach to modeling of composites reinforced by unidirectional fibers is recently presented by Selvadurai and Nikopour [28]. Authors considered the random parallel identical *Carbon fibers* distribution in the *Epoxy matrix* of a composite. In the light of the numerical analysis performed, it is found that in spite of random fibers distribution it is possible to determine a minimal *Representative Area Element*—RAE (>65 fibers number) that guarantees the property of *transversely isotropic symmetry* of *hexagonal* type (5 independent constants in the elasticity matrix, see Fig. 3.1).

Extensive state-of-the-art review of the micromechanics-based analysis of composite materials, enriched by numerous actual results, both in the field of homogenization techniques and its experimental validation for real long-fiber reinforced composites, are found in recently published excellent monograph by Aboudi et al. [1].

3.2 Analogy Between the Elastic Matrices Symmetry at the Level of Crystal Lattice Unit Cell and the Composite Representative Element

A useful analogy between the *crystal lattice symmetry* at the level of single crystal lattice or crystal grains and the relevant microstructure of composite materials of identical symmetry groups that characterize effective elastic matrices (stiffness or compliance) at the macrolevel is sketched in Fig. 3.1.

Equations of linear elasticity of crystal and *composite materials* are written in (3.1)

$$\{\sigma\}^{(cr)} = [\mathfrak{c}] \{\varepsilon\}^{(cr)} \qquad \text{and} \qquad \{\overline{\sigma}\} = [\overline{\mathbb{E}}] \{\overline{\varepsilon}\} \tag{3.1}$$
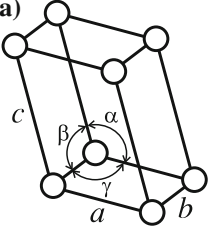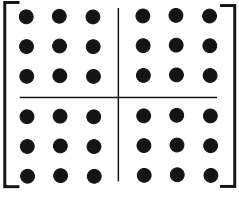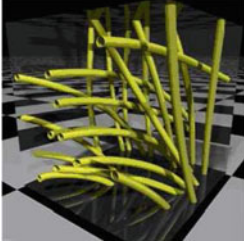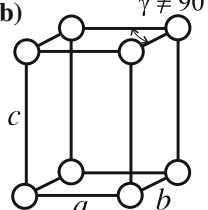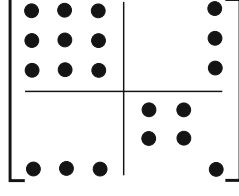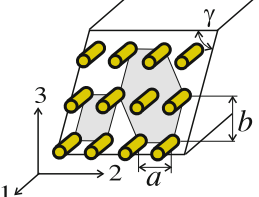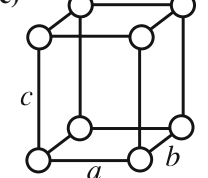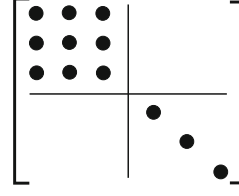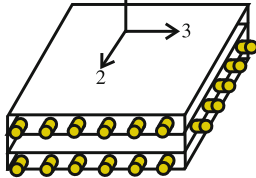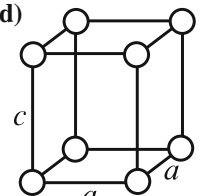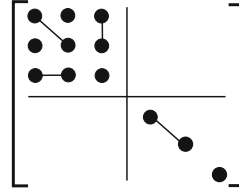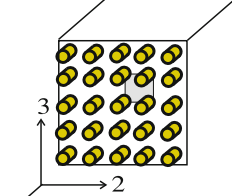
Conventional unit cells of space lattices	Compliance matrix $[\mathbb{E}^{-1}]$	Examplary composits microstructure
(a) $a \neq b \neq c$ $\alpha \neq \beta \neq \gamma$ triclinic lattice	anisotropic Hooke's (21 constants)	anisotropic fibers arrangement in C/C composite (after Martin-Herrero and Germain [21])
(b) $a \neq b \neq c$ $\alpha = \beta = 90°,\ \gamma \neq 90°$ monoclinic lattice	monoclinic or oblique Hooke's anisotropy (13 constants) cf. Nye [23]	rhombic fiber array (after Wúrkner et al [37], Li [17])
(c) $a \neq b \neq c$ $\alpha = \beta = \gamma = 90°$ orthorhombic lattice	orthotropic Hooke's (9 constants)	perpendicular fibers arrangement in multi-laminate plate (2D)
(d) $a = b \neq c$ $\alpha = \beta = \gamma = 90°$ tetragonal lattice	transversely isotropic tetragonal Hooke's (6 constants)	square fiber array (after Sun and Vaidya [30])

Fig. 3.1 Classification of selected composites with respect to the format of compliance matrix $[\mathbb{E}^{-1}]$: **a** anisotropic fiber arrangement, **b** rhombic fiber arrangement, **c** orthotropic fiber arrangement, **d** square fiber arrangement, **e** hexagonal fiber arrangement, **f** regular particle arrangement, **g** random particle arrangement, after Tjong and Ma [33], Martin-Herrero and Germain [21], Nye [23]
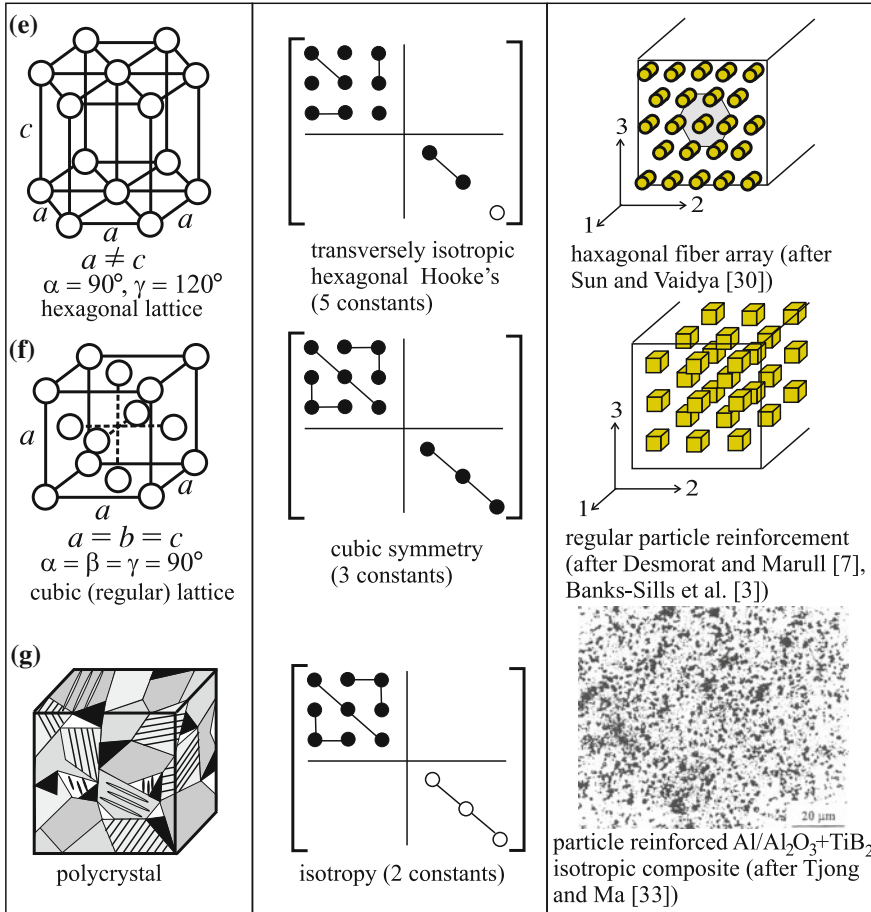
Fig. 3.1 (continued)

where relevant stiffness matrices at the crystal and composite level possessing identical symmetry properties are denoted with $[\mathfrak{s}]$ and $[\mathfrak{c}]$ whereas $\{\boldsymbol{\sigma}\}^{(cr)}$, $\{\boldsymbol{\varepsilon}\}^{(cr)}$, and $\{\overline{\boldsymbol{\sigma}}\}$, $\{\overline{\boldsymbol{\varepsilon}}\}$ stand for stress and strain vectors at the microlevel and the effective stress and strain averaged over the representative element (RVE or RUC) (see Gan et al. [9], Selvadurai and Nikopour [28], etc.). The respective compliance matrices used in Eq. (3.1) can be rewritten in the equivalent fashion

$$\{\varepsilon\}^{(cr)} = [\mathfrak{s}]\{\boldsymbol{\sigma}\}^{(cr)} \qquad \text{and} \qquad \{\overline{\varepsilon}\} = [\overline{\mathbb{E}}^{-1}]\{\overline{\sigma}\} \tag{3.2}$$

where the *effective compliance matrix* is represented as

$$[\overline{\mathbb{E}}^{-1}] = \begin{bmatrix} \overline{E}_{11}^{-1} & \overline{E}_{12}^{-1} & \overline{E}_{13}^{-1} & \overline{E}_{14}^{-1} & \overline{E}_{15}^{-1} & \overline{E}_{16}^{-1} \\ \overline{E}_{21}^{-1} & \overline{E}_{22}^{-1} & \overline{E}_{23}^{-1} & \overline{E}_{24}^{-1} & \overline{E}_{25}^{-1} & \overline{E}_{26}^{-1} \\ \overline{E}_{31}^{-1} & \overline{E}_{32}^{-1} & \overline{E}_{33}^{-1} & \overline{E}_{34}^{-1} & \overline{E}_{35}^{-1} & \overline{E}_{36}^{-1} \\ \overline{E}_{41}^{-1} & \overline{E}_{42}^{-1} & \overline{E}_{43}^{-1} & \overline{E}_{44}^{-1} & \overline{E}_{45}^{-1} & \overline{E}_{46}^{-1} \\ \overline{E}_{51}^{-1} & \overline{E}_{52}^{-1} & \overline{E}_{53}^{-1} & \overline{E}_{54}^{-1} & \overline{E}_{55}^{-1} & \overline{E}_{56}^{-1} \\ \overline{E}_{61}^{-1} & \overline{E}_{62}^{-1} & \overline{E}_{63}^{-1} & \overline{E}_{64}^{-1} & \overline{E}_{65}^{-1} & \overline{E}_{66}^{-1} \end{bmatrix} \tag{3.3}$$

The stiffness and compliance matrices at the crystal level in Eqs. (3.1) and (3.2) are denoted by [𝖈] and [𝖘] in accordance with the notation used in crystallography as shown in Table 3.2.

Compliance matrices are more convenient for further application since they have, generally, simpler representation when compared to the respective stiffness matrices, both expressed in terms of the engineering elasticity constants (*Young modules E_{ii}, Kirchhoff modules G_{ij}, Poisson ratios ν_{ij}, Chencov modules $\mu_{ij(kl)}$ and Rabinovich modules $\eta_{i(jk)}$* as shown in Table 3.1). In a more general case of fully anisotropic composite material, for instance when composite material is at the microlevel reinforced with *Carbon nanotubes* of *irregular arrangement*, the effective continuum of averaged properties is fully anisotropic and characterized by 21 engineering modules where the effective compliance matrix of the composite $[\overline{\mathbb{E}}^{-1}]$ expressed in terms of engineering anisotropy constants is furnished as follows:

$$[\overline{\mathbb{E}}^{-1}] = \begin{bmatrix} \dfrac{1}{E_{11}} & -\dfrac{\nu_{21}}{E_{11}} & -\dfrac{\nu_{31}}{E_{11}} & \dfrac{\eta_{23(1)}}{E_{11}} & \dfrac{\eta_{31(1)}}{E_{11}} & \dfrac{\eta_{12(1)}}{E_{11}} \\ -\dfrac{\nu_{12}}{E_{22}} & \dfrac{1}{E_{22}} & -\dfrac{\nu_{32}}{E_{22}} & \dfrac{\eta_{23(2)}}{E_{22}} & \dfrac{\eta_{31(2)}}{E_{22}} & \dfrac{\eta_{12(2)}}{E_{22}} \\ -\dfrac{\nu_{13}}{E_{33}} & -\dfrac{\nu_{23}}{E_{33}} & \dfrac{1}{E_{33}} & \dfrac{\eta_{23(3)}}{E_{33}} & \dfrac{\eta_{31(3)}}{E_{33}} & \dfrac{\eta_{12(3)}}{E_{33}} \\ \dfrac{\eta_{(1)23}}{G_{23}} & \dfrac{\eta_{(2)23}}{G_{23}} & \dfrac{\eta_{(3)23}}{G_{23}} & \dfrac{1}{G_{23}} & \dfrac{\mu_{31(23)}}{G_{23}} & \dfrac{\mu_{12(23)}}{G_{23}} \\ \dfrac{\eta_{(1)31}}{G_{31}} & \dfrac{\eta_{(2)31}}{G_{31}} & \dfrac{\eta_{(3)31}}{G_{31}} & \dfrac{\mu_{(23)31}}{G_{31}} & \dfrac{1}{G_{31}} & \dfrac{\mu_{12(31)}}{G_{31}} \\ \dfrac{\eta_{(1)12}}{G_{12}} & \dfrac{\eta_{(2)12}}{G_{12}} & \dfrac{\eta_{(3)12}}{G_{12}} & \dfrac{\mu_{(23)12}}{G_{12}} & \dfrac{\mu_{(31)12}}{G_{12}} & \dfrac{1}{G_{12}} \end{bmatrix} \tag{3.4}$$

In Table 3.1 engineering anisotropy constants are ordered into five groups:

- E_{ii}—*axial* elasticity *modules* (three generalized Young modules)
- G_{ij}—*shear modules* at three anisotropy planes (three generalized Kirchhoff modules)
- ν_{ij}—*transverse strain coefficients* (three generalized Poisson ratios)
- $\mu_{ij(kl)}$—*Chencov modules* (three Chencov modules combining shear in different anisotropy planes)
- $\eta_{i(jk)}$—*Rabinovich modules* (nine Rabinovich modules combining shear and normal strain effects).

It is worth to mention that the symmetry of stress and strain tensors results in appropriate symmetry of the compliance (stiffness) matrix, Lekhnitskii [16].

Table 3.1 Types of engineering modules used in representation of the compliance matrix (3.4)

Engineering modules	Coupling effect		Considered axes or planes (coupling)	Number of components
	Stress component	Strain component		
E_{11}, E_{22}, E_{33}	Axial	Axial	Same axes $1 \rightarrow 1$, etc.	3
G_{12}, G_{32}, G_{31}	Shear	Shear	Same planes $12 \rightarrow 12$, etc.	3
$\nu_{21}, \nu_{31}, \nu_{32}$	Axial	Axial	Transverse directions $1 \rightarrow 2$, etc.	3
$\mu_{31(23)}, \mu_{12(23)}, \mu_{12(31)}$	Shear	Shear	Different planes $13 \rightarrow 23$, etc.	3
$\eta_{23(1)}, \ldots, \eta_{12(3)}$	Shear	Axial	Normal to $23 \rightarrow 1$, etc.	9

$$
\begin{aligned}
\frac{\nu_{ij}}{E_{jj}} &= \frac{\nu_{ji}}{E_{ii}} &\longrightarrow \nu_{ij} E_{ii} &= \nu_{ji} E_{jj} \\
\frac{\eta_{ij(k)}}{E_{kk}} &= \frac{\eta_{(k)ij}}{G_{ij}} &\longrightarrow \eta_{ij(k)} G_{ij} &= \eta_{(k)ij} E_{kk} \\
\frac{\mu_{ij(ki)}}{G_{ki}} &= \frac{\mu_{(ki)ij}}{G_{ji}} &\longrightarrow \mu_{ij(ki)} G_{ji} &= \mu_{(ki)ij} G_{ki}
\end{aligned}
\tag{3.5}
$$

A convenient *analogy* between the crystal lattice symmetry, the effective matrix and respective configuration/orientation of fibers or particles in exemplary unit cells of composites is shown in Fig. 3.1. Before we start to discuss items a–g in Fig. 3.1, a comment should be done that an analogy between the exemplary representative composite microstructure and the conventional unit cell of a crystal lattice is built based on the *identical stiffness matrix format* and symmetry properties at the level of crystal unit representative cells (lattice) and the level of composite representative unit cell (fibers/particles geometry, arrangement, etc.), but not on different physical features.

Such analogy occurs to be helpful in proper description of *symmetry groups* and *classes* of the elastic matrices and proposing their experimental-based identification.

In a general case of anisotropy Eq. (3.4), the respective *triclinic crystal lattice symmetry* ensures fully populated stiffness matrices at both levels considered (crystal lattice vs. microstructure) for instance due to the totally *anisotropic Carbon/Carbon composite* (see Fig. 3.1a Martin-Herrero and Germain [21]).

Composites formed by *stacking layers* (lamina) at different fiber orientation are called *laminates*, the effective properties of which vary with orientation, thickness, and stacking sequence of layers. The effective properties of a unidirectional lamina are classified as orthotropic with different properties in the material directions (cf. Herakovich and Aboudi [12]). In general, the effective properties of such
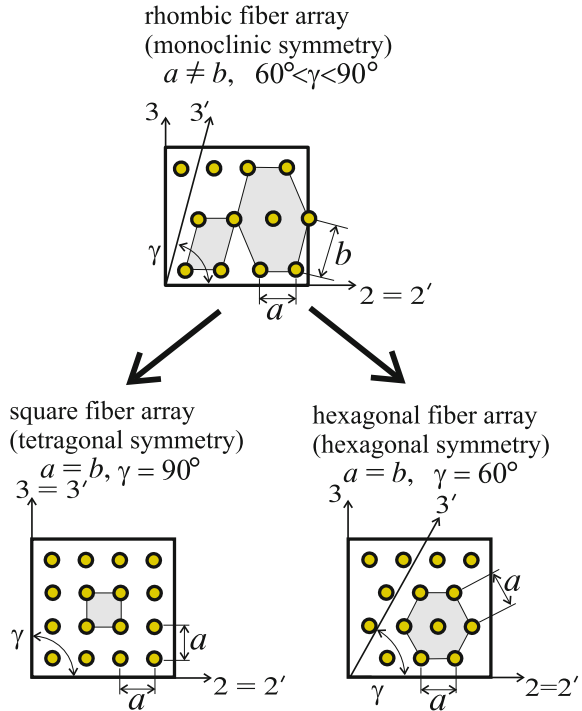
multicomponent systems correspond to *averaged orthotropic continuum* described by nine *orthotropy modules* E_{11}, E_{22}, E_{33}, ν_{21}, ν_{32}, ν_{31}, G_{12}, G_{23}, G_{31}, if elastic range is considered. The corresponding *crystal lattice symmetry* is known as the *orthorhombic* lattice characterized by three different cell edges $a \neq b \neq c$ and identical angles $\alpha = \beta = \gamma = 90°$, Fig. 3.1c.

Unidirectionally reinforced composites with the regular parallel fibers arrangement correspond to the *averaged transversely isotropic continuum* at the macrolevel. However, depending on frequently used periodic fiber arrangements, two of them are specially interesting: *tetragonal (square) fiber array* and *hexagonal fiber array*, as shown in Fig. 3.1d, e, respectively. Corresponding two crystal lattice cells are also presented that exhibit equivalence between the in-plane fiber array over the composite RUC and in-plane atoms in the *Crystal Unit Cell* CUC arrangements. Note that in case of tetragonal transverse isotropy, the number of independent modules is equal to six, whereas in case of hexagonal transverse isotropy this number is reduced to five.

Consider for a moment a more general case called the *monoclinic* or *oblique symmetry*. At the level of *composite RUC* it corresponds to the *rhombic fiber array* as shown in Fig. 3.1b. In this case, periodicity is dependent not only on the distance between layers but also on the angle of slope of the RUC walls $60° < \gamma < 90°$. The corresponding crystal lattice symmetry is known as *monoclinic lattice symmetry*. This case can be recognized as an intermediate between the *triclinic lattice* (Fig. 3.1a) and the *orthorhombic lattice* (Fig. 3.1c). Consequently, the equivalent stiffness matrix describing monoclinic anisotropy is enriched with four nonzeroth independent elements $\overline{E}_{16}^{-1}$, $\overline{E}_{26}^{-1}$, $\overline{E}_{36}^{-1}$, and $\overline{E}_{45}^{-1}$, such that total number of independent modules of the compliance matrix is equal to $13 = 9 + 4$. Presence of these additional elements is a characteristic feature for *Rabinovich constants* $\eta_{(i)jk}$ and *Chencov constants* $\mu_{ij(kl)}$ responsible for anisotropy (which are not present in orthotropy).

Consider further more detailed two particular fiber arrangements of the monoclinic symmetry (Fig. 3.1b) which easily can be recognized in two fiber arrays of the *tetragonal* or the *hexagonal symmetry* appearing in transversely isotropic *long-fiber-reinforced composites*. In both cases, $a = b$ holds but two particular magnitudes of the slope angle a *rhombic array* of γ are admitted: $\gamma = 90°$ or $\gamma = 60°$ (Fig. 3.2). In the first case when $\gamma = 90°$, rhombic fiber array reduces to the *square fiber array* (at the composite level) and the equivalent representative crystal lattice cell exhibits architecture of *tetragonal symmetry*, as previously shown in Fig. 3.1d. In the second case when $\gamma = 60°$, any arbitrary rhombic array reduces to another *hexagonal fiber array* (at the composite level) with the equivalent crystal lattice cell architecture of hexagonal symmetry, see Fig. 3.1d. In both cases considered in the compliance matrix $[\mathbb{E}^{-1}]$ of Eq. (3.4) four elements describing the Rabinovich and the Chencov effects $\overline{E}_{16}^{-1} = \overline{E}_{26}^{-1} = \overline{E}_{36}^{-1} = \overline{E}_{45}^{-1} = 0$ disappear such that only nine elements are present in the *orthotropic Hooke law* Fig. 3.1e. However, in case of transverse isotropy, the number of independent modules reduces to either six (square array, $\gamma = 90°$) or five (hexagonal array, $\gamma = 60°$) since in the last case the in-plane modulus equals $\overline{E}_{66}^{-1} = (\overline{E}_{11}^{-1} - \overline{E}_{12}^{-1})/2$ and should be considered as dependent.

Fig. 3.2 Square or hexagonal fiber arrays as particular cases of rhombic fiber array

rhombic fiber array
(monoclinic symmetry)
$a \neq b, \quad 60° < \gamma < 90°$

square fiber array
(tetragonal symmetry)
$a = b, \gamma = 90°$

hexagonal fiber array
(hexagonal symmetry)
$a = b, \quad \gamma = 60°$

Finally, for the narrower case of the tetragonal lattice namely $a = b = c$ and $\alpha = \beta = \gamma = 90°$ the particular *cubic crystal lattice* is recovered (regular lattice). The stiffness or compliance matrices are here characterized by three independent constants: $E_{11}^{-1} = E_{22}^{-1} = E_{33}^{-1}, E_{12}^{-1} = E_{13}^{-1} = E_{23}^{-1}, E_{44}^{-1} = E_{55}^{-1} = E_{66}^{-1}$ see Fig. 3.1f. Such cubic symmetry case is sometimes expected in certain regular particle arrangement, as discussed by Desmorat and Marull [7] and Banks-Sills et al. [3].

To make this classification complete, the particle-reinforced composites of irregular particle shape and their topology should be admitted. In such a case, at the macrolevel, the properties of *isotropy of composite* inside RUC can be admitted, where two independent elastic constants (effective) can satisfactorily be estimated from the Voigt/Reuss rules based on the particle volume fraction V_f only, see Fig. 3.1g.

In schematic representation of the elastic matrices of crystal lattice and composite microstructure, the visualization of matrix elements was adopted after Nye [23] where ● depicts independent modules, ○ dependent modules, whereas ●—● or ○—○ pairs of identical modules, etc. (see Chap. 2).

As it was aforementioned, a similarity between the symmetry classes of crystals at the crystal lattice level and composite microstructure at the macrolevel has subsidiary meaning only. In fact, the *crystal symmetry* implies format and symmetry of the elastic crystal matrices: stiffness $[\mathfrak{c}_{ij}]$ or compliance $[\mathfrak{s}_{ij}]$ being 2nd rank matrix representation of 4th rank *crystal elasticity tensors* $\mathfrak{c}_{ijkl}$ or $\mathfrak{s}_{ijkl}$. Passing from the

Table 3.2 Equations of elasticity at the crystal level and macrolevel

Notation	Crystal level	Macrolevel
Tensor	$\sigma_{ij}^{(cr)} = \mathfrak{c}_{ijkl}\varepsilon_{kl}^{(cr)}$	$\overline{\sigma}_{ij} = \overline{E}_{ijkl}\overline{\varepsilon}_{kl}$
	$\varepsilon_{ij}^{(cr)} = \mathfrak{s}_{ijkl}\sigma_{kl}^{(cr)}$	$\overline{\varepsilon}_{ij} = \overline{E}_{ijkl}^{-1}\overline{\sigma}_{kl}$
Matrix-vector	$\sigma_i^{(cr)} = \mathfrak{c}_{ij}\varepsilon_j^{(cr)}$	$\overline{\sigma}_j = \overline{E}_{ij}\overline{\varepsilon}_j$
	$\varepsilon_i^{(cr)} = \mathfrak{s}_{ij}\sigma_j^{(cr)}$	$\overline{\varepsilon}_i = \overline{E}_{ij}^{-1}\overline{\sigma}_j$

atomic level (*crystal lattice*) to the *macrolevel* (*composite RUC*), we arrive at the correspondence to the *equivalent composite matrices* $\overline{E}_{ij}$ or $\overline{E}_{ij}^{-1}$ built as equivalent representation matrices (averaged in procedure of homogenization) of the *composite effective elasticity tensors* $\overline{E}_{ijkl}$ or $\overline{E}_{ijkl}^{-1}$, see Table 3.2. It is necessary to distinguish stress and strain at the *atomic crystal lattice level* $\sigma_{ij}^{(cr)}$ and $\varepsilon_{ij}^{(cr)}$ from analogous variables measured at the level of RUC: *macrostress* and *macrostrain* $\overline{\sigma}_{ij}$ and $\overline{\varepsilon}_{ij}$. Note that in crystallography, components of tensors $\mathfrak{c}_{ijkl}$ and $\mathfrak{s}_{ijkl}$ are traditionally called the *stiffness coefficients* and the *compliance coefficients*. On the other hand, when passing to the macrolevel of analysis, the effective tensor components of composite $\overline{E}_{ijkl}$ and $\overline{E}_{ijkl}^{-1}$ are named stiffness and compliance constants. Mention that there does not exist any direct correspondence between elastic crystal coefficients and the effective elastic constants of composite material at the macrolevel, c.f. Nye [23]. Remember also that during the fabrication process of composite, the residual thermal stresses different in matrix and fibers material have to be built-in into enriched equations of elasticity. Assuming for simplicity that during the fabrication process strains have elastic nature only, the application of conventional equations of thermoelasticity is justified. However, during the final cooling down process of the composite and also in the fabrication phase, some thermoplastic microstructure change in the material can be observed. In such cases, the thermoelastic analysis may occur incorrect (cf. e.g., Herakovich and Aboudi [12]).

3.3 Effective Elastic Matrix Characterization of Composites with Various Symmetries

3.3.1 Triclinic Anisotropic Long-Fiber-Reinforced Composite (Anisotropic Fiber Array, Fig. 3.1a)

Elasticity equation of anisotropic composite material (at the macroscale) written in an arbitrary material frame can be furnished in a following fashion, cf. Eq. (3.4)

$$
\begin{Bmatrix}
\bar{\varepsilon}_{11} \\
\bar{\varepsilon}_{22} \\
\bar{\varepsilon}_{33} \\
\bar{\gamma}_{23} \\
\bar{\gamma}_{31} \\
\bar{\gamma}_{12}
\end{Bmatrix}
=
\left[
\begin{array}{ccc|ccc}
\frac{1}{E_{11}} & -\frac{\nu_{21}}{E_{11}} & -\frac{\nu_{31}}{E_{11}} & \frac{\eta_{23(1)}}{E_{11}} & \frac{\eta_{31(1)}}{E_{11}} & \frac{\eta_{12(1)}}{E_{11}} \\
-\frac{\nu_{12}}{E_{22}} & \frac{1}{E_{22}} & -\frac{\nu_{32}}{E_{22}} & \frac{\eta_{23(2)}}{E_{22}} & \frac{\eta_{31(2)}}{E_{22}} & \frac{\eta_{12(2)}}{E_{22}} \\
-\frac{\nu_{13}}{E_{33}} & -\frac{\nu_{23}}{E_{33}} & \frac{1}{E_{33}} & \frac{\eta_{23(3)}}{E_{33}} & \frac{\eta_{31(3)}}{E_{33}} & \frac{\eta_{12(3)}}{E_{33}} \\
\frac{\eta_{(1)23}}{G_{23}} & \frac{\eta_{(2)23}}{G_{23}} & \frac{\eta_{(3)23}}{G_{23}} & \frac{1}{G_{23}} & \frac{\mu_{31(23)}}{G_{23}} & \frac{\mu_{12(23)}}{G_{23}} \\
\frac{\eta_{(1)31}}{G_{31}} & \frac{\eta_{(2)31}}{G_{31}} & \frac{\eta_{(3)31}}{G_{31}} & \frac{\mu_{(23)31}}{G_{31}} & \frac{1}{G_{31}} & \frac{\mu_{12(31)}}{G_{31}} \\
\frac{\eta_{(1)12}}{G_{12}} & \frac{\eta_{(2)12}}{G_{12}} & \frac{\eta_{(3)12}}{G_{12}} & \frac{\mu_{(23)12}}{G_{12}} & \frac{\mu_{(31)12}}{G_{12}} & \frac{1}{G_{12}}
\end{array}
\right]
\begin{Bmatrix}
\bar{\sigma}_{11} \\
\bar{\sigma}_{22} \\
\bar{\sigma}_{33} \\
\bar{\tau}_{23} \\
\bar{\tau}_{31} \\
\bar{\tau}_{12}
\end{Bmatrix}
\tag{3.6}
$$

Taking into account the symmetry conditions of the effective compliance matrix $\overline{E}_{ij}^{-1} = \overline{E}_{ji}^{-1}$, see Eq. (3.5), in order to completely determine fully populated 6×6 matrix of elasticity total number of required elements is equal to $n = \frac{(1+6)6}{2} = 21$. However, following the reasoning of Lekhnitskii [16] and others, the maximal number of different from zero but independent matrix elements $\overline{E}_{ij}^{-1}$ equals 18 (see Table 3.1). It follows from requirement that both *effective compliance* $\overline{E}_{ij}^{-1}$ and *stiffness* $\overline{E}_{ij}$ *matrices* have to obey transformation rule by three Euler angles. In such general case of anisotropy, that in crystallography corresponds to *triclinic lattice symmetry*, it is impossible to reduce to zero any matrix elements via some transformation by a rotation of the reference frame with any angles.

3.3.2 Monoclinic or Oblique Anisotropic Long-Fiber Composite (Rhombic Fiber Array, Fig. 3.1b)

Composite systems of the *rhombic*-type *fiber architecture* represent the particular case of generally anisotropic composite geometry in such manner as the *monoclinic crystal lattice symmetry* is the particular case of general *triclinic symmetry* at the crystal lattice level. In such rhombic-type fiber array composites, the axis parallel to the fibers direction can be distinguished (3) being perpendicular to the transverse plane (1, 2). Corresponding equation of elasticity built on the base of *oblique anisotropy compliance matrix* takes the following format

$$
\begin{Bmatrix}
\bar{\varepsilon}_{11} \\
\bar{\varepsilon}_{22} \\
\bar{\varepsilon}_{33} \\
\bar{\gamma}_{23} \\
\bar{\gamma}_{31} \\
\bar{\gamma}_{12}
\end{Bmatrix}
=
\left[
\begin{array}{ccc|ccc}
\frac{1}{E_{11}} & -\frac{\nu_{21}}{E_{11}} & -\frac{\nu_{31}}{E_{11}} & & & \frac{\eta_{12(1)}}{E_{11}} \\
-\frac{\nu_{12}}{E_{22}} & \frac{1}{E_{22}} & -\frac{\nu_{32}}{E_{22}} & & & \frac{\eta_{12(2)}}{E_{22}} \\
-\frac{\nu_{13}}{E_{33}} & -\frac{\nu_{23}}{E_{33}} & \frac{1}{E_{33}} & & & \frac{\eta_{12(3)}}{E_{33}} \\
 & & & \frac{1}{G_{23}} & \frac{\mu_{31(23)}}{G_{23}} & \\
 & & & \frac{\mu_{(23)31}}{G_{31}} & \frac{1}{G_{31}} & \\
\frac{\eta_{(1)12}}{G_{12}} & \frac{\eta_{(2)12}}{G_{12}} & \frac{\eta_{(3)12}}{G_{12}} & & & \frac{1}{G_{12}}
\end{array}
\right]
\begin{Bmatrix}
\bar{\sigma}_{11} \\
\bar{\sigma}_{22} \\
\bar{\sigma}_{33} \\
\bar{\tau}_{23} \\
\bar{\tau}_{31} \\
\bar{\tau}_{12}
\end{Bmatrix}
\tag{3.7}
$$

By contrast to generally anisotropic composite matrix Eq. (3.6), in the case of composite of *oblique anisotropy property* number of nonzeroth independent material

structural modules equals 13. Among them: three *Young modules* E_{11}, E_{22}, E_{33}; three *Kirchhoff modules* G_{23}, G_{31}, G_{12}; three *Poisson ratios* $\nu_{21}, \nu_{31}, \nu_{32}$; one *Chencov modulus* $\mu_{31(23)}$; and three *Rabinovich modules* $\eta_{12(1)}, \eta_{12(2)}, \eta_{12(3)}$ are present in Eq. (3.7) instead of 21 (18 irreducible) shown in Eq. 3.6. On the other hand, appearance of some Chencov $\mu_{31(23)}$ and Rabinovich $\eta_{12(k)}$ coefficients allows to distinguish formats of the compliance matrices in case of the *rhombic fiber array* in which neither Rabinovoch nor Chencov coefficients are present, when the material orthotropy frame coincides with the effective stress/strain frame.

3.3.3 Orthotropic Composite (Lamina with Perpendicular Fiber Arrangement, Fig. 3.1c)

The narrower case of frequently used composites built of a number of layers which are long-fiber reinforced in an alternate perpendicular layer after layer fashion are called the *orthotropic multi-laminate composites*, commonly also named lamina. In corresponding elasticity matrices, compliance or stiffness, Rabinovich $\eta_{12(k)}$ and Chencov $\mu_{31(23)}$ coefficients (present in previously discussed Eq. 3.7) disappear in Eq. (3.8) such that the number of independent modules of the *effective elastic compliance* $\overline{E}_{ij}^{-1}$ or *stiffness matrix* $\overline{E}_{ij}$ is reduced to $9 = 13 - 4$, namely: 3 *Young modules* E_{11}, E_{22}, E_{33}; 3 *Kirchhoff modules* G_{23}, G_{31}, G_{12}; 3 *Poisson ratios* $\nu_{21}, \nu_{31}, \nu_{32}$. These equivalent anisotropy constants of composite have to be either measured in appropriate 9 tests or estimated by the use of a chosen homogenization method for assumed *perpendicular fiber arrangements* (see for instance Gan et al. [9] for Boron/Al composite)

$$\begin{Bmatrix} \overline{\varepsilon}_{11} \\ \overline{\varepsilon}_{22} \\ \overline{\varepsilon}_{33} \\ \overline{\gamma}_{23} \\ \overline{\gamma}_{31} \\ \overline{\gamma}_{12} \end{Bmatrix} = \begin{bmatrix} \frac{1}{E_{11}} & -\frac{\nu_{21}}{E_{11}} & -\frac{\nu_{31}}{E_{11}} & & & \\ -\frac{\nu_{12}}{E_{22}} & \frac{1}{E_{22}} & -\frac{\nu_{32}}{E_{22}} & & & \\ -\frac{\nu_{13}}{E_{33}} & -\frac{\nu_{23}}{E_{33}} & \frac{1}{E_{33}} & & & \\ & & & \frac{1}{G_{23}} & & \\ & & & & \frac{1}{G_{31}} & \\ & & & & & \frac{1}{G_{12}} \end{bmatrix} \begin{Bmatrix} \overline{\sigma}_{11} \\ \overline{\sigma}_{22} \\ \overline{\sigma}_{33} \\ \overline{\tau}_{23} \\ \overline{\tau}_{31} \\ \overline{\tau}_{12} \end{Bmatrix} \quad (3.8)$$

Transformation of the relation $\{\varepsilon\} = \left[\mathbb{E}^{-1}\right]\{\sigma\}$ to $\{\sigma\} = [\mathbb{E}]\{\varepsilon\}$ is not a trivial one in case of the elastic orthotropy. It can be done in a numerical fashion by finding the *stiffness matrix* $[\mathbb{E}]$ which is inverse to the *compliance matrix* $\left[\mathbb{E}^{-1}\right]$. Elements of the stiffness matrix $[\mathbb{E}]$ can be explicitly expressed in terms of nine *engineering constants of orthotropic material* determined $E_{11}, E_{22}, E_{33}, G_{23}, G_{13}, G_{12}, \nu_{21}, \nu_{31}$ and ν_{32} as follows (see Ochoa and Reddy [24], Tamma and Avila [32])

$$
\begin{Bmatrix}
\overline{\sigma}_{11} \\
\overline{\sigma}_{22} \\
\overline{\sigma}_{33} \\
\overline{\sigma}_{23} \\
\overline{\sigma}_{31} \\
\overline{\sigma}_{12}
\end{Bmatrix}
=
\begin{bmatrix}
E_{1111} & E_{1122} & E_{1133} & & & \\
E_{2211} & E_{2222} & E_{2233} & & & \\
E_{3311} & E_{3322} & E_{3333} & & & \\
& & & E_{2323} & & \\
& & & & E_{1313} & \\
& & & & & E_{1212}
\end{bmatrix}
\begin{Bmatrix}
\overline{\varepsilon}_{11} \\
\overline{\varepsilon}_{22} \\
\overline{\varepsilon}_{33} \\
\overline{\gamma}_{23} \\
\overline{\gamma}_{31} \\
\overline{\gamma}_{12}
\end{Bmatrix}
\tag{3.9}
$$

where subsequent elements of the stiffness matrix $[\mathbb{E}]$ are given by equations

$$
\begin{aligned}
E_{1111} &= \frac{1-\nu_{23}\nu_{32}}{\Delta} E_{11} & E_{1122} &= \frac{\nu_{12}+\nu_{13}\nu_{32}}{\Delta} E_{22} \\
E_{1133} &= \frac{\nu_{13}+\nu_{12}\nu_{23}}{\Delta} E_{33} & E_{2222} &= \frac{1-\nu_{13}\nu_{31}}{\Delta} E_{22} \\
E_{2233} &= \frac{\nu_{23}+\nu_{21}\nu_{13}}{\Delta} E_{33} & E_{3333} &= \frac{1-\nu_{12}\nu_{21}}{\Delta} E_{33} \\
E_{2323} &= G_{23} & E_{1313} = G_{13} \qquad & E_{1212} = G_{12}
\end{aligned}
\tag{3.10}
$$

whereas symbol Δ denotes

$$
\Delta = 1 - \nu_{12}\nu_{21} - \nu_{13}\nu_{31} - \nu_{23}\nu_{32} - \nu_{12}\nu_{23}\nu_{31} - \nu_{21}\nu_{13}\nu_{32}
\tag{3.11}
$$

Note that full orthotropic symmetry and population of both matrices stiffness (3.9) and compliance (3.8) is saved and refers to appropriate combinations of engineering constants but not to engineering constants separately, for instance

$$
E_{1122} = \frac{\nu_{21}+\nu_{13}\nu_{32}}{\Delta} E_{22} = \frac{\nu_{12}+\nu_{31}\nu_{23}}{\Delta} E_{11} = E_{2211} \qquad \text{etc.}
\tag{3.12}
$$

Hence only nine *orthotropy modules* are independent.

3.3.4 Unidirectional Long-Fiber Composite—Transversely Isotropic Tetragonal Type (Square Fiber Array, Fig. 3.1d)

Particular case of orthotropic composite is *transversely isotropic symmetry* unidirectional long-fiber-reinforced system in which fibers are built-in with the regular *tetragonal* manner (*square fiber array*, Fig. 3.1d). The effective elasticity matrix of such composite is described with six independent constants: E_{11}, E_{33}, ν_{21}, ν_{32}, G_{23} and G_{12} as shown in Eq. (3.13). At the level of RUC, tetragonal symmetry is observed (4 in-plane axes)

$$\begin{Bmatrix} \bar{\varepsilon}_{11} \\ \bar{\varepsilon}_{22} \\ \bar{\varepsilon}_{33} \\ \bar{\gamma}_{23} \\ \bar{\gamma}_{31} \\ \bar{\gamma}_{12} \end{Bmatrix} = \begin{bmatrix} \frac{1}{E_{11}} & -\frac{\nu_{21}}{E_{11}} & -\frac{\nu_{21}}{E_{11}} & & & \\ -\frac{\nu_{12}}{E_{22}} & \frac{1}{E_{22}} & -\frac{\nu_{32}}{E_{22}} & & & \\ -\frac{\nu_{12}}{E_{22}} & -\frac{\nu_{23}}{E_{22}} & \frac{1}{E_{22}} & & & \\ & & & \frac{1}{G_{23}} & & \\ & & & & \frac{1}{G_{12}} & \\ & & & & & \frac{1}{G_{12}} \end{bmatrix} \begin{Bmatrix} \bar{\sigma}_{11} \\ \bar{\sigma}_{22} \\ \bar{\sigma}_{33} \\ \bar{\tau}_{23} \\ \bar{\tau}_{31} \\ \bar{\tau}_{12} \end{Bmatrix} \qquad (3.13)$$

3.3.5 Unidirectional Long-Fiber Composite—Transversely Isotropic Hexagonal Type (Hexagonal Fiber Array Fig. 3.1e)

In the another case of *unidirectionally reinforced composites*, when in the system fibers are row after row shifted by the half-distance, at the level of RUC the *hexagonal symmetry* property holds (six symmetry axes). Hence, only five from among mechanical constants are independent, since $G_{23} = \frac{E_{22}}{2(1+\nu_{23})}$

$$\begin{Bmatrix} \bar{\varepsilon}_{11} \\ \bar{\varepsilon}_{22} \\ \bar{\varepsilon}_{33} \\ \bar{\gamma}_{23} \\ \bar{\gamma}_{31} \\ \bar{\gamma}_{12} \end{Bmatrix} = \begin{bmatrix} \frac{1}{E_{11}} & -\frac{\nu_{21}}{E_{11}} & -\frac{\nu_{21}}{E_{11}} & & & \\ -\frac{\nu_{12}}{E_{22}} & \frac{1}{E_{22}} & -\frac{\nu_{32}}{E_{22}} & & & \\ -\frac{\nu_{12}}{E_{22}} & -\frac{\nu_{23}}{E_{22}} & \frac{1}{E_{22}} & & & \\ & & & \frac{2(1+\nu_{23})}{E_{22}} & & \\ & & & & \frac{1}{G_{12}} & \\ & & & & & \frac{1}{G_{12}} \end{bmatrix} \begin{Bmatrix} \bar{\sigma}_{11} \\ \bar{\sigma}_{22} \\ \bar{\sigma}_{33} \\ \bar{\tau}_{23} \\ \bar{\tau}_{31} \\ \bar{\tau}_{12} \end{Bmatrix} \qquad (3.14)$$

The two types of transversely isotropic composites dependent on the fiber arrangement of either tetragonal or hexagonal symmetry are not always consistently examined which may lead to some erroneous conclusions (cf. Sun and Vaidya [30]).

3.3.6 Regular Particle-Reinforced Composite—Cubic Symmetry (Regular Particles Arrangement, Fig. 3.1f)

It is commonly assumed that the composites reinforced with a randomly distributed particles of irregular size and shape can be treated at the level of RVE as the isotropic continuum. However, in case of some *regular particle reinforcement* by repeating identical shape and size particles, the equivalent composite continuum exhibits the *cubic symmetry* (Fig. 3.1f). Among the crystal materials of cubic (regular) symmetry long list can be mentioned: Pyrites (cubic), Fluor Spar, Rock-salt, Potassium

Chloride (cf. Love [20]) or Tantalum, Aluminum, Gold, Copper, Germanium, α–iron, Magnesium Oxide (Magnesia), and Spinel ($MgAl_2O_4$) (cf. Berryman [5]). All cubic symmetry materials are characterized by three independent compliance modules: $\overline{E}_{11}^{-1}$, $\overline{E}_{12}^{-1}$ and $\overline{E}_{44}^{-1}$ where $\overline{E}_{44}^{-1} \neq (\overline{E}_{11}^{-1} - \overline{E}_{12}^{-1})/2$ or equivalently $G \neq \frac{E}{2(1+\nu)}$. In a similar way, the composite reinforced with three-directional mutually perpendicular short-fiber of the cubic symmetry is described by three independent engineering constants E, ν, and G

$$
\begin{Bmatrix} \overline{\varepsilon}_{11} \\ \overline{\varepsilon}_{22} \\ \overline{\varepsilon}_{33} \\ \overline{\gamma}_{23} \\ \overline{\gamma}_{31} \\ \overline{\gamma}_{12} \end{Bmatrix} = \begin{bmatrix} \frac{1}{E} & -\frac{\nu}{E} & -\frac{\nu}{E} & & & \\ -\frac{\nu}{E} & \frac{1}{E} & -\frac{\nu}{E} & & & \\ -\frac{\nu}{E} & -\frac{\nu}{E} & \frac{1}{E} & & & \\ & & & \frac{1}{G} & & \\ & & & & \frac{1}{G} & \\ & & & & & \frac{1}{G} \end{bmatrix} \begin{Bmatrix} \overline{\sigma}_{11} \\ \overline{\sigma}_{22} \\ \overline{\sigma}_{33} \\ \overline{\tau}_{23} \\ \overline{\tau}_{31} \\ \overline{\tau}_{12} \end{Bmatrix}
\tag{3.15}
$$

3.3.7 Isotropic Composite (Random Particle Arrangement, Fig. 3.1g)

Irregular particle-reinforced composite in which the distribution shape and orientation of particles are fully disordered (chaotic) can be described at the level of the repeating RVE by the effective elasticity matrix (stiffness or compliance) characterized by two independent modules: $\overline{E}_{11}^{-1}$, $\overline{E}_{12}^{-1}$ ($\overline{E}_{44}^{-1} = (\overline{E}_{11}^{-1} - \overline{E}_{12}^{-1})/2$ or equivalently $G = \frac{E}{2(1+\nu)}$). In the *isotropic composite* with irregular particle reinforcement, no characteristic material frame can be distinguished inside RVE (infinite number of symmetry axes)

$$
\begin{Bmatrix} \overline{\varepsilon}_{11} \\ \overline{\varepsilon}_{22} \\ \overline{\varepsilon}_{33} \\ \overline{\gamma}_{23} \\ \overline{\gamma}_{31} \\ \overline{\gamma}_{12} \end{Bmatrix} = \begin{bmatrix} \frac{1}{E} & -\frac{\nu}{E} & -\frac{\nu}{E} & & & \\ -\frac{\nu}{E} & \frac{1}{E} & -\frac{\nu}{E} & & & \\ -\frac{\nu}{E} & -\frac{\nu}{E} & \frac{1}{E} & & & \\ & & & \frac{2(1+\nu)}{E} & & \\ & & & & \frac{2(1+\nu)}{E} & \\ & & & & & \frac{2(1+\nu)}{E} \end{bmatrix} \begin{Bmatrix} \overline{\sigma}_{11} \\ \overline{\sigma}_{22} \\ \overline{\sigma}_{33} \\ \overline{\tau}_{23} \\ \overline{\tau}_{31} \\ \overline{\tau}_{12} \end{Bmatrix}
\tag{3.16}
$$

More general approach to describe particle-reinforced composites in which size/shape and topology of particles are ordered with the specific symmetries may lead to various symmetry classes of elastic matrices (cf. Banks-Sills et al. [3]).

3.4 Bounds for Effective Elastic Properties of Unidirectionally (Long Fiber) Reinforced Composites of Tetragonal or Hexagonal Symmetry

3.4.1 Nature of Homogenization Problem in Modeling of Heterogeneous Composites—Voigt and Reuss' Concept

Composite materials described in Sect. 3.3 have to be considered as two- or multi-component systems at the microlevel (microcomposites) or the nanolevel (nanocomposites). Composite materials are in essence nonhomogeneous or in fact *heterogeneous materials* due to different properties of the system constituents (components) commonly recognized as the *matrix* (most frequently *metallic*, *ceramic* or *polymer*) and the *reinforcing fibers* or *particles* (for instance long fibers made of *ceramic* or *metallic materials* and others) although the constituent materials are essentially homogeneous. At microscale, on boundaries between the components of different materials a jump of mechanical, thermal, and other properties arise. Averaging methods inside the *representative element* (RVE) or the representative cell (RUC) used for analysis of *multicomponent composite materials* known as *homogenization methods* are based on the assumption that it is possible to determine approximate values of the effective properties of the equivalent homogeneous composite (heterogeneous in fact) as well as uniform macrostress and macrostrain (nonuniform in fact at the microlevel), cf. Fig. 3.3. It is necessary to accept existence of the repeating *Representative Volume Element*—RVE (cf. e.g., Sun and Vaidya [30], Gan et al. [9], Würkner et al. [37], Bayat and Aghdam [4]), or the Representative Unit Cell—RUC
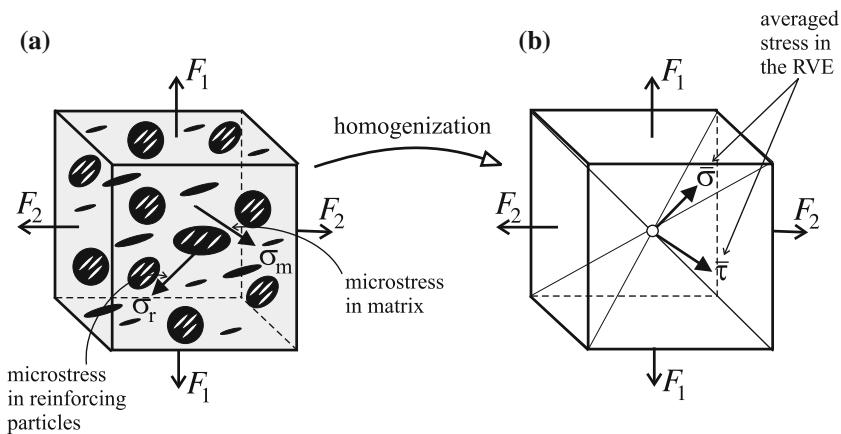

Fig. 3.3 Representative volume element RVE: **a** heterogeneous material at microscale, **b** homogeneous material at macroscale

(cf. e.g., Li and Wongsto [18], Li [17], Wongsto and Li [36], Pidaparti and May [26], Banks-Sills et al. [3], Herakovich and Aboudi [12]) which are subsequently divided into the subcells, Fig. 3.5. The RVE size or the RUC size and geometry have to be sufficiently large in order to properly catch an essence of composite system properties and behavior at the macroscale. Simultaneously, they have to be sufficiently small but repeatedly noticeable to assure that the representation of a uniform deformation field described by the displacement $\boldsymbol{u}$ and the gradient $\nabla\boldsymbol{u}$ such that the averaged (effective) strain $\overline{\boldsymbol{\varepsilon}} = \frac{1}{2}(\nabla^{\mathrm{T}}\boldsymbol{u} + \nabla\boldsymbol{u})$ is justified (cf. Gan et al. [9]). Note that component material at the microlevel (or nanolevel) is usually isotropic; however, a multiphase composite can be either isotropic (for majority of particular composites) or anisotropic (for instance in case of fibrous composites reinforced with directionally oriented fiber beam).

The differences between the RVE (Representative Volume Element) and RUC (Repeating Unit Cell) concept are discussed in details by Drago and Pindera [8]. The authors claim that the concept of RVE is addressed to the statistically homogeneous material at an appropriate scale. Moreover it is assumed that the strain and stress are uniform throughout the RVE. On the other hand Drago and Pindera assume the periodicity in the material, both in strain and stress fields. However most researchers assume that the RUC is the periodic RVE and use its interchangeably [1, 30].

Traditionally it is assumed that the *particle-reinforced composites* in a disordered manner (e.g., with dispersed micro or nanoparticles as well as short micro or nanowires) show isotropic symmetry after homogenization (at the level of RVE). However, the above reasoning has to be accepted with necessary care. If repeatable shape and regular orientation of reinforcing particles are ensured throughout the matrix volume, in spite of the isotropic properties of both phases—*matrix* and *reinforcement* it may happen that after homogenization the averaged material modules at the macroscale (composite level) exhibit other than isotropic symmetry properties. Such problem was analyzed by Banks-Sills et al. [3] with respect to the *Glass-Epoxy composite*, by the use for simulation particles of various but regular geometries: spherical, cylindrical, cubic and rectangular parallelepiped. To be more precise the following unusual remark can be cited: "An interesting surprise for rotated particles was the existence of unusual material constants which cause normal deformations to produce orthogonal shear stresses and vice versa effect of Rabinovich's coefficients and shear deformations to produce orthogonal shear stresses and vice versa effect of Chencov's coefficients", cf. Banks-Sills et al. [3].

Only in the specific case if reinforcing particles are repeatedly spherical and do not exhibit same characteristic spatial distribution the assumption about isotropic symmetry at the macroscale (RVE-level) is reasonable to accept. In such specific case the classical mixture rules can be applied in order to achieve averaging methods: the *Voigt* [34] or the *Reuss estimates* [27]. In the simplest case of two isotropic constituent phase materials, Voigt and Reuss' *rules of mixture* are simply based on the volume fraction of matrix V_1 and reinforcement V_2

$$^\text{V}\overline{p} = p_1 c_1 + p_2 c_2 \quad \text{Voigt's rule}$$

$$\frac{1}{^\text{R}\overline{p}} = \frac{c_1}{p_1} + \frac{c_2}{p_2} \qquad \text{Reuss' rule} \tag{3.17}$$

Symbols p_1 and p_2 stand for elastic constants of constituent materials, matrix and reinforcement (particles), for instance Young modules E_1 and E_2 and Kirchhoff modules G_1 and G_2 whereas $^\text{V}\overline{p}$ and $^\text{R}\overline{p}$ denote the corresponding effective modules $\overline{E}$ and $\overline{G}$ averaged at the RVE level. Symbols c_1 and c_2 stand for *volume fraction* of both phases (V_f and $1 - V_\text{f}$) with *irregular particles distribution* throughout the RVE ignoring effect of local concentration density, size and shape of particles and their orientation and mutual interaction, see Fig. 3.3a. After homogenization, the *averaged* (effective) *stress* $\overline{\sigma}$ and $\overline{\tau}$ are met in RVE instead of different *microstresses* in constituent materials: matrix σ_m and reinforcement σ_r (see Fig. 3.3b).

The mixture rules Voigt and Reuss' (3.17) lead to different estimates of averaged material constants of homogenized isotropic continuum $\overline{E}$ and $\overline{G}$. In case of *Voigt estimate* compatibility of strains in both phase materials is assumed, whereas in case of *Reuss' estimate* compatibility of stresses is postulated. The first approach leads to discontinuity of stress at the boundary between constituents whereas the second approach causes strain discontinuity. In other words, the Voigt approximation can be treated as equivalent to kinematically admissible approach in contrast to the Reuss approximation which is statically admissible. In fact at the microlevel of *heterogeneous composite* both stress and strain continuity hold such that the Voigt and the Reuss approximations can serve as *upper* and *lower estimates* for the *effective stiffness matrix* elements of anisotropic composite systems (cf. Herakovich [11], Gan et al. [9]). In the impressive monograph "Micromechanics of composite materials," Aboudi et al. [1] analyze the effective engineering constants of the Glass/Epoxy fibrous composite $E_{11}, E_{22} = E_{33}, \nu_{12} = \nu_{13}, \nu_{23}, G_{12} = G_{13}, G_{23}$ as functions of fiber volume fraction V_f. This findings generally confirm the upper and lower bounds by Voigt and Reuss' isotropic estimates except for the transverse Poisson ratio ν_{23} for which an excess of the bounds is observed.

In order to simply explain the essence of Voigt and Reuss' estimates, consider elementary one-dimensional two-component mechanical systems sketched in Fig. 3.4 representing: (a) Voigt, (b) Reuss' and (c) the effective homogeneous elements.

In case of *Voigt scheme*, Fig. 3.4a, two bars of A_1 and A_2 cross-sectional areas that represent matrix and reinforcement (particle) of the same length l are jointed in parallel ($\overline{l} = l_1 = l_2$ and $\overline{A} = A_1 + A_2$). Loading force F is separated between matrix and reinforcement $F = F_1 + F_2$ whereas identical elongation of both constituents is equal to the averaged elongation of substituting homogeneous system, Fig. 3.4c: $\Delta\overline{l} = \Delta l_1 = \Delta l_2$. Hence, when the Hooke law is applied to schemes a) and c) we arrive at distribution of force between matrix and reinforcement

$$F_1 = \frac{E_1 A_1}{\overline{E}(A_1 + A_2)}F \qquad F_2 = \frac{E_2 A_2}{\overline{E}(A_1 + A_2)}F \tag{3.18}$$
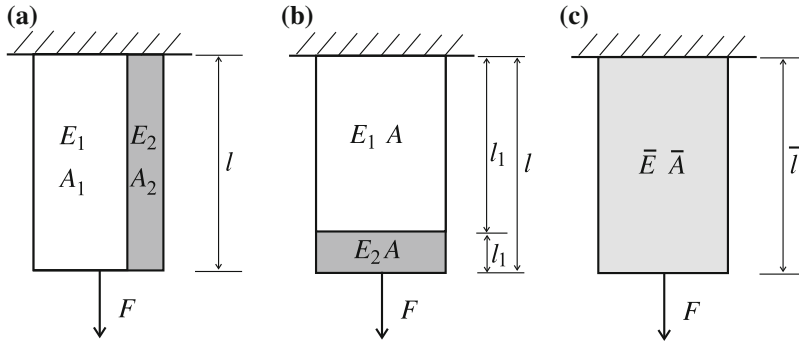
Fig. 3.4 Uniaxial mechanical models for mixture rules application in composites: **a** Voigt rule, **b** Reuss' rule, **c** effective homogeneous material

Finally, introducing definitions of volume fractions $V_1 = A_1/\overline{A}$ and $V_2 = A_2/\overline{A}$ the Voigt-based effective Young modulus $^V\overline{E}$ is furnished

$$\overline{E} = E_1 V_1 + E_2 V_2 = \ ^V\overline{E} \tag{3.19}$$

In case of *Reuss' scheme*, Fig. 3.4b, two bars of different lengths l_1 and l_2 and $A_1 = A_2 = \overline{A}$ representing matrix and reinforcement materials are joined in series and loaded by identical force $F = F_1 = F_2$ whereas averaged elongation of substitutive system Fig. 3.4c is the sum of component elongations $\Delta\overline{l} = \Delta l_1 + \Delta l_2$. Again, when Hooke law is applied to schemes (b) and (c) the following must hold

$$\frac{F\overline{l}}{\overline{E}\,\overline{A}} = \frac{Fl_1}{E_1\overline{A}} + \frac{Fl_2}{E_2\overline{A}} \tag{3.20}$$

Finally applying definitions of volume fractions $V_1 = l_1/\overline{l}$ and $V_2 = l_2/\overline{l}$ we arrive at the Reuss-based effective Young modulus $^R\overline{E}$ in the format

$$\frac{1}{\overline{E}} = \frac{V_1}{E_1} + \frac{V_2}{E_2} = \frac{1}{^R\overline{E}} \tag{3.21}$$

In order to make further considerations easier we introduce original notation used by Hill in [13]. In this way equations describing the *uniaxial Voigt and Reuss' models* can be rewritten in the new following formats. In case of Voigt model the identity of strains in both phases $^V\overline{\varepsilon} = \varepsilon_1 = \varepsilon_2$ holds. Hence the following set of equations describe the uniaxial Voigt model

$$
\begin{aligned}
{}^{\mathrm{V}}\overline{\sigma} &= {}^{\mathrm{V}}c_1\sigma_1 + {}^{\mathrm{V}}c_2\sigma_2 \\
{}^{\mathrm{V}}\overline{\sigma} &= {}^{\mathrm{V}}\overline{E}\,{}^{\mathrm{V}}\overline{\varepsilon} \\
{}^{\mathrm{V}}\overline{E}\,{}^{\mathrm{V}}\overline{\varepsilon} &= {}^{\mathrm{V}}c_1 E_1\varepsilon_1 + {}^{\mathrm{V}}c_2 E_2\varepsilon_2 \\
{}^{\mathrm{V}}\overline{E} &= {}^{\mathrm{V}}c_1 E_1 + {}^{\mathrm{V}}c_2 E_2
\end{aligned}
\tag{3.22}
$$

where fractional concentrations by volume of the phases in the Voigt model (see Fig. 3.4a) are defined as ${}^{\mathrm{V}}c_1 = A_1/\overline{A}$ and ${}^{\mathrm{V}}c_2 = A_2/\overline{A}$; $({}^{\mathrm{V}}c_1 + {}^{\mathrm{V}}c_2 = 1)$.

In the analogous way in case of *uniaxial Reuss' model* the identity of stresses in both phases ${}^{\mathrm{R}}\overline{\sigma} = \sigma_1 = \sigma_2$ holds, hence the basic set of equations is

$$
\begin{aligned}
{}^{\mathrm{R}}\overline{\varepsilon} &= {}^{\mathrm{R}}c_1\varepsilon_1 + {}^{\mathrm{R}}c_2\varepsilon_2 \\
{}^{\mathrm{R}}\overline{\varepsilon} &= \frac{{}^{\mathrm{R}}\overline{\varepsilon}}{{}^{\mathrm{R}}\overline{E}} \\
\frac{{}^{\mathrm{R}}\overline{\sigma}}{{}^{\mathrm{R}}\overline{E}} &= {}^{\mathrm{R}}c_1\frac{\sigma_1}{E_1} + {}^{\mathrm{V}}c_2\frac{\sigma_2}{E_2} \\
\frac{1}{{}^{\mathrm{R}}\overline{E}} &= \frac{{}^{\mathrm{R}}c_1}{E_1} + \frac{{}^{\mathrm{R}}c_2}{E_2}
\end{aligned}
\tag{3.23}
$$

where fractional concentrations by volume of the phases in the Reuss model (see Fig. 3.4b) are defined as ${}^{\mathrm{R}}c_1 = l_1/\overline{l}$ and ${}^{\mathrm{R}}c_2 = l_2/\overline{l}$; $({}^{\mathrm{R}}c_1 + {}^{\mathrm{R}}c_2 = 1)$.

In fact both pairs ${}^{\mathrm{V}}c_1$, ${}^{\mathrm{V}}c_2$ and ${}^{\mathrm{R}}c_1$, ${}^{\mathrm{R}}c_2$ can be interpreted as common volume fraction of both phases V_{f} and $1 - V_{\mathrm{f}}$ in the uniaxial models of the same material, hence it must hold

$$
c_1 = {}^{\mathrm{V}}c_1 = {}^{\mathrm{R}}c_1 = V_{\mathrm{f}} \qquad c_2 = {}^{\mathrm{V}}c_2 = {}^{\mathrm{R}}c_2 = 1 - V_{\mathrm{f}}
\tag{3.24}
$$

Note that the Poisson effect is ignored in aforementioned considerations.

3.4.2 General 3D Formulation of Voigt and Reuss' Homogenization Estimates

On the RVE level, that represents heterogeneous material, the definitions of either the *averaged stress* or the *averaged strain* tensors can be written down

$$
\overline{\sigma} = \frac{1}{V_{\mathrm{RVE}}} \int_{V_{\mathrm{RVE}}} \sigma \, dV
\tag{3.25}
$$

or

$$
\overline{\varepsilon} = \frac{1}{V_{\mathrm{RVE}}} \int_{V_{\mathrm{RVE}}} \varepsilon \, dV
\tag{3.26}
$$

where V_{RVE} denotes a *volume of* the chosen *RVE*, see Aboudi et al. [1].

Average values of stress and strain $\overline{\sigma}$ and $\overline{\varepsilon}$ in RVE are given in terms of $\overline{\sigma}_1$, $\overline{\sigma}_2$ and $\overline{\varepsilon}_1$, $\overline{\varepsilon}_2$ in the phases by the following relations

$$\overline{\sigma} = c_1\overline{\sigma}_1 + c_2\overline{\sigma}_2 \qquad \overline{\varepsilon} = c_1\overline{\varepsilon}_1 + c_2\overline{\varepsilon}_2 \tag{3.27}$$

Since the elastic material is assumed for both phases the obvious relations must hold at any point in the phases

$$\sigma_1 = \mathbb{E}_1 : \varepsilon_1 \quad \text{and} \quad \sigma_2 = \mathbb{E}_2 : \varepsilon_2 \tag{3.28}$$

and

$$\varepsilon_1 = \mathbb{E}_1^{-1} : \sigma_1 \quad \text{and} \quad \varepsilon_2 = \mathbb{E}_2^{-1} : \sigma_2 \tag{3.29}$$

if the inverse format is used.

Substitution of (3.28) and (3.29) into (3.27) with the assumption that phases are uniform and isotropic ($\sigma_{1,2} = \overline{\sigma}_{1,2}, \varepsilon_{1,2} = \overline{\varepsilon}_{1,2}$) the analogous relations hold between the average quantities

$$\overline{\sigma} = c_1\mathbb{E}_1 : \overline{\varepsilon}_1 + c_2\mathbb{E}_2 : \overline{\varepsilon}_2 \qquad \overline{\varepsilon} = c_1\mathbb{E}_1^{-1} : \overline{\sigma}_1 + c_2\mathbb{E}_2^{-1} : \overline{\sigma}_2 \tag{3.30}$$

where consistently $\overline{\varepsilon}_1$ and $\overline{\varepsilon}_2$, as well as $\overline{\sigma}_1$ and $\overline{\sigma}_2$, stand for uniform strain and uniform stress fields in each of the phases in RVE, respectively.

A distribution of the two-phase materials in the RVE is obviously not necessarily random, but must be *structurally representative distribution* for composite material at the *macrolevel*. In the light of above remark a unique relationship between the *average strains in* the *phases* $\overline{\varepsilon}_1$, $\overline{\varepsilon}_2$ upon the *average overall strain in RVE* $\overline{\varepsilon}$ can be furnished by the use of *strain concentration tensors* $\mathbb{A}_1$ and $\mathbb{A}_2$

$$\overline{\varepsilon}_1 = \mathbb{A}_1 : \overline{\varepsilon} \qquad \overline{\varepsilon}_2 = \mathbb{A}_2 : \overline{\varepsilon} \tag{3.31}$$

where the obvious condition holds $c_1\mathbb{A}_1 + c_2\mathbb{A}_2 = \mathbb{I}$ with $\mathbb{I}$ being the *unit tensor*. By combining Eq. (3.31) with Eq. (3.30) we arrive at

$$\overline{\sigma} = (c_1\mathbb{E}_1 : \mathbb{A}_1 + c_2\mathbb{E}_2 : \mathbb{A}_2) : \overline{\varepsilon} = \overline{\overline{\mathbb{E}}} : \overline{\varepsilon} \tag{3.32}$$

where $\overline{\overline{\mathbb{E}}}$ stands for the effective stiffness tensor of the overall composite.

Equivalently reverse unique relationships between the *average stresses in* the *phases* $\overline{\sigma}_1$, $\overline{\sigma}_2$ upon the *average stress in RVE* $\overline{\sigma}$

$$\overline{\sigma}_1 = \mathbb{B}_1 : \overline{\sigma} \qquad \overline{\sigma}_2 = \mathbb{B}_2 : \overline{\sigma} \tag{3.33}$$

must hold if the *stress concentration tensors* $\mathbb{B}_1$ and $\mathbb{B}_2$ which satisfy the relation $c_1\mathbb{B}_1 + c_2\mathbb{B}_2 = \mathbb{I}$, are introduced. Again combining Eq. (3.33) with the second of Eq. (3.30) we arrive at

$$\overline{\varepsilon} = (c_1 \mathbb{E}_1^{-1} : \mathbb{B}_1 + c_2 \mathbb{E}_2^{-1} : \mathbb{B}_2) : \overline{\sigma} = \overline{\mathbb{E}}^{-1} : \overline{\sigma} \qquad (3.34)$$

where $\overline{\mathbb{E}}^{-1}$ is the *effective compliance tensor of* the *composite*.

The first homogenization rule was introduced by Voigt (1889) [34] as average constants of polycrystals. Assuming the strain concentration is constant $\mathbb{A}_1 = \mathbb{A}_2 = \mathbb{I}$ and *strain is uniform* $\overline{\varepsilon}_1 = \overline{\varepsilon}_2 = \overline{\varepsilon}$, it follows:

$$\overline{\mathbb{E}} = c_1 \mathbb{E}_1 + c_2 \mathbb{E}_2 \qquad (3.35)$$

Equation (3.35) provides the *effective stiffness matrix* elements *of* the *composite* in terms of the *volume-averaged stiffness* of individual phases.

By contrast, Reuss (1929) [27] assumed that constituents of the composite are subjected to a *uniform stress* equal to the *average stress in RVE* $\mathbb{B}_1 = \mathbb{B}_2 = \mathbb{I}$ in Eq. (3.33) and effective compliance is given by a rule of mixture as follows:

$$\overline{\mathbb{E}}^{-1} = c_1 \mathbb{E}_1^{-1} + c_2 \mathbb{E}_2^{-1} \qquad (3.36)$$

Note that in fact neither the Voigt nor the Reuss assumption is correct. The implied stress due to Voigt causes tractions at phase boundaries not satisfying equilibrium $\overline{\sigma}_1 \neq \overline{\sigma}_2$. On the other hand the implied strain due to Reuss' causes discontinuity of strain at the interface between matrix and particle $\overline{\varepsilon}_1 \neq \overline{\varepsilon}_2$.

3.4.3 Theorem of Lower and Upper Bounds by Voigt and Reuss' Estimation

Hill theorem, which is called the *theorem of lower and upper bounds*, allows to connect a constitutive description at two scales: *micro level* at the point level and the *meso level*, where the representative volume element RVE is defined. After Auriault et al. [2], it is assumed that:

- the *global variables* are the volume means of the local stress and strains, and that the conservation and constitutive equations have the same structure at microscopic and mesoscales,
- the assumption of *energetic consistency*, known as the Hill principle, which imposes equality on the energy contained within the medium, whether it is expressed in local variables or using variables defined at mesoscale.

According to the second assumption, the *equivalence of energy* at micro and RVE level leads to the following formula:

$$\int\limits_V \sigma : \varepsilon \mathrm{d}V = \int\limits_V \overline{\sigma} : \overline{\varepsilon} \mathrm{d}V = V \overline{\sigma} : \overline{\varepsilon} \qquad (3.37)$$

where $V = V_{\text{RVE}}$ is used for brevity. Hence, when the Hooke law is applied, both at micro level $\boldsymbol{\sigma} = \mathbb{E} : \boldsymbol{\varepsilon}$ and mesoscale $\overline{\boldsymbol{\sigma}} = \overline{\mathbb{E}} : \overline{\boldsymbol{\varepsilon}}$, the previous equation can be rewritten as

$$\int\limits_{V} \boldsymbol{\varepsilon} : \mathbb{E} : \boldsymbol{\varepsilon} \, dV = V \overline{\boldsymbol{\varepsilon}} : \overline{\mathbb{E}} : \overline{\boldsymbol{\varepsilon}} \tag{3.38}$$

According to the *Hill–Mandel relation* and Eq. (3.37) the following equality holds:

$$\overline{\boldsymbol{\sigma}} : \overline{\boldsymbol{\varepsilon}} = \left(\frac{1}{V}\int\limits_{V} \boldsymbol{\sigma} dV\right) : \left(\frac{1}{V}\int\limits_{V} \boldsymbol{\varepsilon} dV\right) = \frac{1}{V}\int\limits_{V} \boldsymbol{\sigma} : \boldsymbol{\varepsilon} dV = (\overline{\boldsymbol{\sigma} : \boldsymbol{\varepsilon}}) \tag{3.39}$$

Let us consider the Representative Volume Element bounded by surface S in which uniform strain field $\overline{\boldsymbol{\varepsilon}} = \text{const}$ accompanies linear displacement field $\boldsymbol{u} = \overline{\boldsymbol{\varepsilon}} \cdot \boldsymbol{x}$, hence the external work can be rewritten down as follows:

$$L_z = \frac{1}{2}\int\limits_{S} \boldsymbol{t} \cdot \boldsymbol{u} dS = \frac{1}{2}\int\limits_{S} \boldsymbol{t} \cdot \overline{\boldsymbol{\varepsilon}} \cdot \boldsymbol{x} dS = \frac{1}{2}\overline{\boldsymbol{\varepsilon}} \cdot \int\limits_{S} \boldsymbol{t} \cdot \boldsymbol{x} dS \tag{3.40}$$

Applying the traction boundary condition in following form $\boldsymbol{t} = \boldsymbol{\sigma} \cdot \boldsymbol{n}$, where $\boldsymbol{n}$ stands for a normal vector to the surface, and the Gauss theorem of divergence, the Eq. (3.40) can be rewritten as follows:

$$L_z = \frac{1}{2}\overline{\boldsymbol{\varepsilon}} \cdot \int\limits_{V} \text{div}\,(\boldsymbol{\sigma} \cdot \boldsymbol{x}) \, dV = \frac{1}{2}\overline{\boldsymbol{\varepsilon}} \cdot \int\limits_{V} [\text{div}\,(\boldsymbol{\sigma}) \cdot \boldsymbol{x} + \boldsymbol{\sigma} \cdot \text{div}(\boldsymbol{x})] \, dV \tag{3.41}$$

The uniform stress accompanying the uniform strain leads to $\text{div}(\boldsymbol{\sigma}) = 0$ hence the external work (3.41) reduces to

$$L_z = \frac{1}{2}\overline{\boldsymbol{\varepsilon}} \cdot \int\limits_{V} \boldsymbol{\sigma} dV = \frac{1}{2}\overline{\boldsymbol{\sigma}} : \overline{\boldsymbol{\varepsilon}} = \frac{1}{2}(\overline{\boldsymbol{\sigma} : \boldsymbol{\varepsilon}}) \tag{3.42}$$

when the Hill–Mandel relation is applied. Applying assumption, that the constitutive relations at both scales are the same:

$$\overline{\boldsymbol{\sigma}} = \overline{\mathbb{E}} : \overline{\boldsymbol{\varepsilon}}, \qquad \boldsymbol{\sigma} = \mathbb{E} : \boldsymbol{\varepsilon} \tag{3.43}$$

the Eq. (3.42) can be rewritten as follows:

$$\overline{\boldsymbol{\sigma}} : \overline{\boldsymbol{\varepsilon}} = (\overline{\boldsymbol{\sigma} : \boldsymbol{\varepsilon}}) = \frac{1}{V}\int\limits_{V} \boldsymbol{\varepsilon} : \mathbb{E} : \boldsymbol{\varepsilon} dV = \overline{\boldsymbol{\varepsilon}} : \overline{\mathbb{E}} : \overline{\boldsymbol{\varepsilon}} \tag{3.44}$$

Let us defined a new *fictitious stress* field $\widehat{\boldsymbol{\sigma}}$, where the Hooke law can be defined as:

$$\widehat{\boldsymbol{\sigma}} = \mathbb{E} : \overline{\boldsymbol{\varepsilon}} \qquad (3.45)$$

The real, effective fields (e.g., stress $\boldsymbol{\sigma}$ and strain $\boldsymbol{\varepsilon}$) must fulfil the *theorem of minimal potential energy*, hence the energy based on a fictitious stress field $\widehat{\boldsymbol{\sigma}}$ must be greater than effective one, so the following inequality is true:

$$(\overline{\boldsymbol{\sigma} : \boldsymbol{\varepsilon}}) = \frac{1}{V} \int_V \boldsymbol{\sigma} : \boldsymbol{\varepsilon} \mathrm{d}V \leq \frac{1}{V} \int_V \widehat{\boldsymbol{\sigma}} : \overline{\boldsymbol{\varepsilon}} \mathrm{d}V \qquad (3.46)$$

Input of the Eq. (3.44) to the left-hand side of above inequality and the definition of fictitious stress (3.45) on the right-hand side, yields the inequality:

$$\frac{1}{V} \int_V \boldsymbol{\varepsilon} : \mathbb{E} : \boldsymbol{\varepsilon} \mathrm{d}V = \overline{\boldsymbol{\varepsilon}} : \overline{\mathbb{E}} : \overline{\boldsymbol{\varepsilon}} \leq \int_V \overline{\boldsymbol{\varepsilon}} : \mathbb{E} : \overline{\boldsymbol{\varepsilon}} \mathrm{d}V = \overline{\boldsymbol{\varepsilon}} : \overline{\boldsymbol{\varepsilon}} : \left(\frac{1}{V} \int_V \mathbb{E} \mathrm{d}V \right) \quad (3.47)$$

After some rearrangements the inequality (3.47) can be rewritten as follows:

$$\overline{\mathbb{E}} \leq \frac{1}{V} \int_V \mathbb{E} \mathrm{d}V \qquad (3.48)$$

Inequality (3.48) means that the *effective stiffness tensor on RVE* level is the *lower bound of mean constitutive tensor* on micro level, where the mean operation is calculated over the volume of Representative Volume Element.

Consider the two-phase continuum, where the total volume of RVE is a sum of two volumes $V = V_1 \cup V_2$. Next, it is assumed that for the both phases constitutive law is Hooke equation, where the material behavior is defined by the tensors $\mathbb{E}_1$ and $\mathbb{E}_2$. Hence it is possible to change the continuous formulation described by Eq. (3.48) to the discrete form as follows, compare (3.32):

$$\overline{\mathbb{E}} \leq c_1 \mathbb{E}_1 + c_2 \mathbb{E}_2 = {}^{\mathrm{V}}\overline{\mathbb{E}} \qquad (3.49)$$

where $c_1 = V_1/V$, $c_2 = V_2/V$ and $c_1 + c_2 = 1$. The right-hand side of above equation is well-known relation called *Voigt estimation*, which means that Voigt formula is a *lower bound of* the *effective stiffness matrix* components.

On the other hand it is assumed that across entire boundary S the uniform boundary conditions $\boldsymbol{t} = \overline{\boldsymbol{\sigma}} \cdot \boldsymbol{n}$ hold, where $\overline{\boldsymbol{\sigma}}$ is a uniform stress in the representative volume RVE. In this case the *work of external forces* is as follows

$$L_z = \frac{1}{2} \int\limits_S \boldsymbol{t} \cdot \boldsymbol{u} \mathrm{d}S = \frac{1}{2} \int\limits_S \overline{\boldsymbol{\sigma}} \cdot \boldsymbol{n} \cdot \boldsymbol{u} \mathrm{d}S \tag{3.50}$$

Consider the theorem of divergence:

$$L_z = \frac{1}{2} \overline{\boldsymbol{\sigma}} : \int\limits_V \frac{1}{2} \left(\nabla \boldsymbol{u} + \nabla^T \boldsymbol{u} \right) \mathrm{d}V = \frac{1}{2} \overline{\boldsymbol{\sigma}} : \int\limits_V \varepsilon \mathrm{d}V = \frac{1}{2} \overline{\boldsymbol{\sigma}} : \overline{\varepsilon} \tag{3.51}$$

According to Eq. (3.44) and substituting Hooke law $\overline{\varepsilon} = \mathbb{E}^{-1} : \overline{\boldsymbol{\sigma}}$ the work of internal forces can be evaluated as follows:

$$\int\limits_V \boldsymbol{\sigma} : \varepsilon \mathrm{d}V = V \overline{\boldsymbol{\sigma}} : \overline{\varepsilon} = V \overline{\boldsymbol{\sigma}} : \overline{\mathbb{E}}^{-1} : \overline{\boldsymbol{\sigma}} \tag{3.52}$$

Consider now a new *fictitious strain* field $\widehat{\varepsilon} = \overline{\mathbb{E}}^{-1} : \boldsymbol{\sigma}$ defined in an analogous fashion as fictitious stress (3.45). On the base of theorem of minimum of potential energy, the inequality as follows must be true:

$$\int\limits_V \boldsymbol{\sigma} : \varepsilon \mathrm{d}V = V \overline{\boldsymbol{\sigma}} : \varepsilon \leq \int\limits_V \overline{\boldsymbol{\sigma}} : \widehat{\varepsilon} \mathrm{d}V \tag{3.53}$$

According to Hooke law applied to the term of right-hand side in above equation and taking into account uniform stress $\overline{\boldsymbol{\sigma}}$, it can be evaluated, compare (3.47):

$$\overline{\mathbb{E}}^{-1} \leq \frac{1}{V} \int\limits_V \mathbb{E}^{-1} \mathrm{d}V \tag{3.54}$$

Consider a similar continuum like previous one, where the whole volume of RVE is a sum of two volumes $V = V_1 \cup V_2$. Next, it is assumed that for the both phases constitutive law is Hooke equation, where the material behavior is defined by the tensors $\mathbb{E}_1$ and $\mathbb{E}_2$. Therefore it is possible to change the continuous formulation described by Eq. (3.54) to discrete form as follows, compare (3.49):

$$\overline{\mathbb{E}}^{-1} \leq c_1 \mathbb{E}_1^{-1} + c_2 \mathbb{E}_2^{-1} = {}^R \overline{\mathbb{E}}^{-1} \tag{3.55}$$

where $c_1 = V_1/V$, $c_2 = V_2/V$ and $c_1 + c_2 = 1$. The right-hand side of above equation is well-known relation called *Reuss' estimation*, which means that Reuss' formula is a *lower bound of* the *effective compliance matrix* components, or equivalently the *upper bound of* the elements of the *effective stiffness matrix*, because the product $\overline{\mathbb{E}} : \overline{\mathbb{E}}^{-1}$ is equal identity tensor $\mathbb{I}$.

3.5 Micromechanics-Based Homogenization Methods

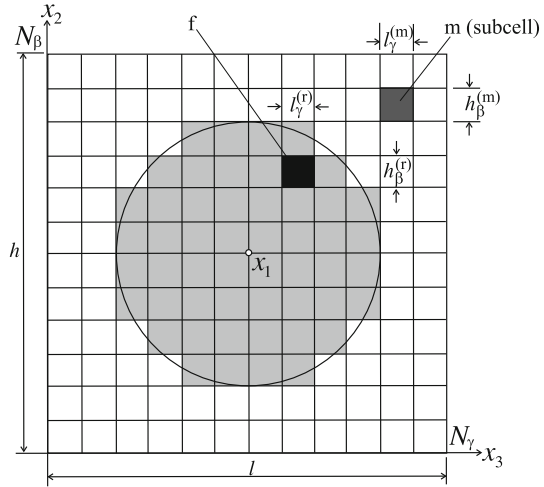### 3.5.1 Effective Elastic Stiffness Matrices of Unidirectional Composites

It is incorrect to directly apply the Voigt and the Reuss rules to anisotropic composites since these simple isotropic mixture rules are based on volume fraction of matrix and reinforcement materials V_m and V_r, but not on true constituents geometry and topology. Hence, Voigt and Reuss' approximations are insufficient for correct estimation of the effective modules of stiffness or compliance matrices of true composite system, for instance with *long-fiber-reinforced composite architecture* of various symmetry. Temporary *micromechanics-based homogenization models* take into account not only the volume fraction of constituents, but also their configuration, geometry and other factors such as *built-in residual stresses* due to fabrication methods. Among them the following homogenization methods are frequently used: the method of *Concentric Cylinder Assembly* (CCA), Hashin and Rosen [10], the *Mori–Tanaka Method* (MT), Mori and Tanaka [22], the *Generalized Method of Cells* (GMC), Paley and Aboudi [25] or *Strain Compatible Method of Cells* (SCMC), Gan et al. [9]. Not going deeply in details, all micromechanics based homogenization methods assume existence of periodically repeating *Representative Volume Element* (RVE) or *Representative Unit Cell* (RUC) the size and geometry of which must capture the essence of the true composite behavior on the macroscale, and which can be mapped into a point of a homogeneous continuum characterized by the displacement field $\boldsymbol{u}$ and the gradient $\nabla \boldsymbol{u}$. Two common GMC and SCMC assumptions are: displacements continuity inside the cell and across the subcell boundaries, and constant strain within the subcells $\boldsymbol{\varepsilon}^{(\beta\gamma)}$, Fig. 3.5. However, by contrast to SCMC method the GMC method does not account for coupling between the transverse shear stresses and the transverse normal stresses, cf. Gan et al. [9]. However, both *microstresses* and *microstrains* averaged at the RUC level $\overline{\sigma}$ and $\overline{\varepsilon}$ are periodical and repeatable at the macroscale (cf. Sun and Vaidya [30]).

Exemplary 2D cross-section of the square representative unit cell hl of *unidirectionally long-fiber-reinforced composite* with RUC domain lh divided into subcells built of different material $h_\beta^{(k)} l_\gamma^{(k)}$, where $k = $ m and $k = $ r stand for matrix and reinforcing fiber, is presented in Fig. 3.5. At the subcell level $h_\beta l_\gamma$ the *local elasticity equation* holds combining local variables in the subcell, *microstrain* $\boldsymbol{\varepsilon}^{(\beta\gamma)}$ and *microstress* $\boldsymbol{\sigma}^{(\beta\gamma)}$

$$\sigma_{ij}^{(\beta\gamma)} = E_{ijkl}^{(\beta\gamma)} \varepsilon_{kl}^{(\beta\gamma)} \tag{3.56}$$

where $E_{ijkl}^{(\beta\gamma)}$ denotes *local stiffness tensor in subcell* $(\beta\gamma)$, different for the matrix material $E_{ijkl}^{(m)}$ and the reinforcing fiber material $E_{ijkl}^{(r)}$. Effective strain $\overline{\varepsilon}_{ij}$ and effective stress $\overline{\sigma}_{ij}$ averaged inside RUC are defined by approximate equations

Fig. 3.5 2D (x_2, x_3 plane) dicretization of the RUC cross-section in unidirectional composite of fiber direction coincident with x_1 direction with size $h \times l$ divided into subcells $h_\beta^{(m)} l_\gamma^{(m)}$ (matrix) and $h_\beta^{(r)} l_\gamma^{(r)}$ (single fiber) of *circular shape* approximated by sufficiently dense *square* subcells

$$\bar{\varepsilon}_{ij} = \frac{1}{hl} \sum_{\beta=1}^{N_\beta} \sum_{\gamma=1}^{N_\gamma} h_\beta l_\gamma \varepsilon_{ij}^{(\beta\gamma)}$$

$$\bar{\sigma}_{ij} = \frac{1}{hl} \sum_{\beta=1}^{N_\beta} \sum_{\gamma=1}^{N_\gamma} h_\beta l_\gamma \sigma_{ij}^{(\beta\gamma)}$$

(3.57)

When the inverse formulas for local variables are taken from (3.57), namely $\varepsilon_{ij}^{(\beta\gamma)}(\bar{\varepsilon}_{ij})$ and $\sigma_{ij}^{(\beta\gamma)}(\bar{\sigma}_{ij})$, and substituted next to local equation of elasticity (3.56) at subcell we arrive at the equation of elasticity at RUC level that combines average stress and average strain

$$\bar{\sigma}_{ij} = \underbrace{\frac{1}{hl} \sum_{\beta=1}^{N_\beta} \sum_{\gamma=1}^{N_\gamma} h_\beta l_\gamma E_{ijkl}^{(\beta\gamma)} A_{klmn}^{(\beta\gamma)}}_{\bar{E}_{ijmn}} \bar{\varepsilon}_{mn}$$

(3.58)

where A_{klmn} is so called tensorial concentration operator the components of which $A_{klmn}^{(\beta\gamma)}$ allow to separate properties of constitutive material matrix and reinforcement (fiber). If the new definition $\bar{E}_{ijmn}$ over RUC for averaged stiffness tensor is introduced (cf. Eq. 3.58) the *averaged elasticity equation in RUC* is furnished

$$\bar{\sigma}_{ij} = \bar{E}_{ijmn} \bar{\varepsilon}_{mn}$$

(3.59)

Note that in the averaged elasticity equation (3.59) $\bar{E}_{klmn}$ stands for effective stiffness tensor of composite expressed in terms of the local elasticity tensors in subcells $\mathbb{E}^{(\beta\gamma)}$ and the concentration tensor $A_{klmn}^{(\beta\gamma)}$ represented by the matrix of concentration factors

Table 3.3 Local and averaged elasticity equations

Notation	Subcell level ($\beta\gamma$)	RUC level
Index	$\sigma_{ij}^{\beta\gamma} = E_{ijkl}^{\beta\gamma}\varepsilon_{kl}^{\beta\gamma}$	$\overline{\sigma}_{ij} = \overline{E}_{ijkl}\overline{\varepsilon}_{kl}$
	$\varepsilon_{ij}^{\beta\gamma} = E_{ijkl}^{-1\beta\gamma}\sigma_{kl}^{\beta\gamma}$	$\overline{\varepsilon}_{ij} = \overline{E}_{ijkl}^{-1}\overline{\sigma}_{kl}$
Vector/matrix	$\{\sigma^{(\beta\gamma)}\} = [\mathbb{E}^{(\beta\gamma)}]\{\varepsilon^{(\beta\gamma)}\}$	$\{\overline{\sigma}\} = [\overline{\mathbb{E}}]\{\overline{\varepsilon}\}$
	$\{\varepsilon^{(\beta\gamma)}\} = [\mathbb{E}^{(\beta\gamma)}]^{-1}\{\sigma^{(\beta\gamma)}\}$	$\{\overline{\varepsilon}\} = [\overline{\mathbb{E}}^{-1}]\{\overline{\sigma}\}$

defining distribution of constituent materials (subcell level) over the RUC (composite level).

If the *vector/matrix notation* is used and the homogenized stiffness matrix is defined in RUC both Eqs. (3.56) and (3.59) can be rewritten in format shown in Table 3.3.

3.5.2 Effective Stiffness Matrices of Unidirectional Composites Characterized by Regular Fiber Configuration—Square Array Versus Hexagonal Array

Final format of the *effective elastic stiffness matrix of composite* $\overline{\mathbb{E}}$ depends not only on the selected homogenization method (for instance Reuss', Voigt, GMC, SCMC etc.) but also on a choice of the *Representative Unit Cell* RUC. In fact a proper choice of RUC geometry should follow true fiber topology in the considered composite. Two basic regular fiber arrays repeating (periodic) at the macroscale of the unidirectional composite are of particular interest: the *square array* and the *hexagonal array* (Fig. 3.6). The rhombic array (Fig. 3.2) is not commonly used in practice, and it will not be considered here.

In case of *tetragonal symmetry* (square array) fibers are arranged in parallel rows and series being equally spaced by distance *a* in the matrix material of composite (Fig. 3.6a). Such fiber configuration in unidirectional composite is used by Tamma and Avila [32], Würkner et al. [37] and others. By contrast, in case of *hexagonal symmetry* (hexagonal array) fibers are distributed in position of parallel rows equally spaced with distance *a* but neighboring rows are shifted each to the other with distance $a/2$ (Fig. 3.6b). Hexagonal symmetry fiber topology is used for example by Herakovich and Aboudi [12], Sun and Vaidya [30] and other authors. Configuration of fibers in composite at the macroscale is a starting point for appropriate selection of the Representative Unit Cell (RUC) geometry for numerical simulation employed by the use of homogenization methods in order to find the effective properties of a composite.

When either the tetragonal or the hexagonal symmetry fiber configurations are employed various Representative Unit Cells can be defined (cf. Sun and Vaidya [30] and others).
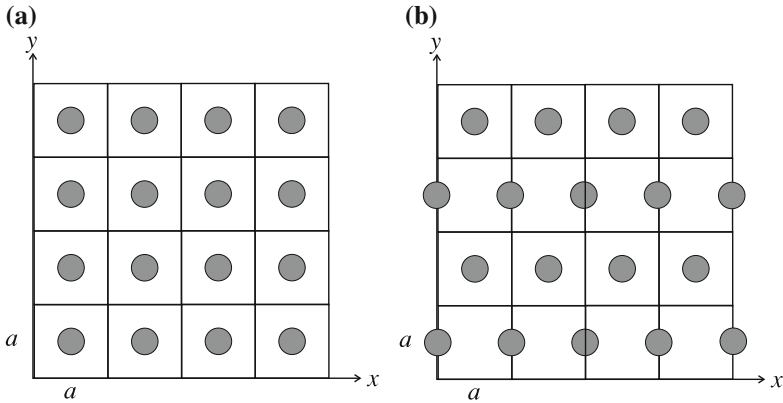
Fig. 3.6 Two configurations of fibers in unidirectionally reinforced transversely isotropic composite (macroscale): **a** tetragonal symmetry, **b** hexagonal symmetry
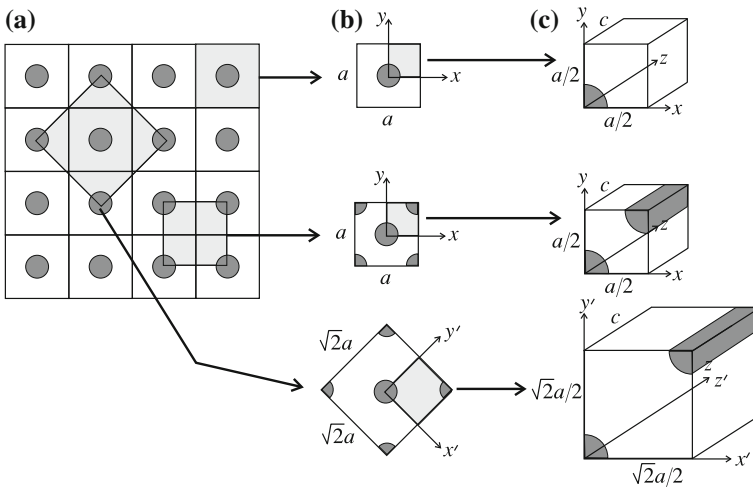

Fig. 3.7 Representative Unit Cells (RUCs) of tetragonal symmetry (square fiber array): **a** various choices of repeating RUCs at the macrolevel, **b** three shape geometires and fiber dispositions in RUCs, **c** three sub-RUCs and fiber geometry with additional symmetry used

In case of the fibers topology that exhibits *tetragonal symmetry* (*square fiber arrays*, Fig. 3.7a) three different representative unit cells are used (see Fig. 3.7b, c). Due to the transverse isotropy property, in fact the 2D analysis is sufficient whereas the choice of one of the three cells presented in Fig. 3.7c for numerical simulation is insignificant.

On the other hand if the fibers topology is governed by the *hexagonal symmetry* (*hexagonal arrays*), Fig. 3.8a, the other two Representative Unit Cells can be established as shown in Fig. 3.8b. Note that the *RUCs of the tetragonal symmetry*
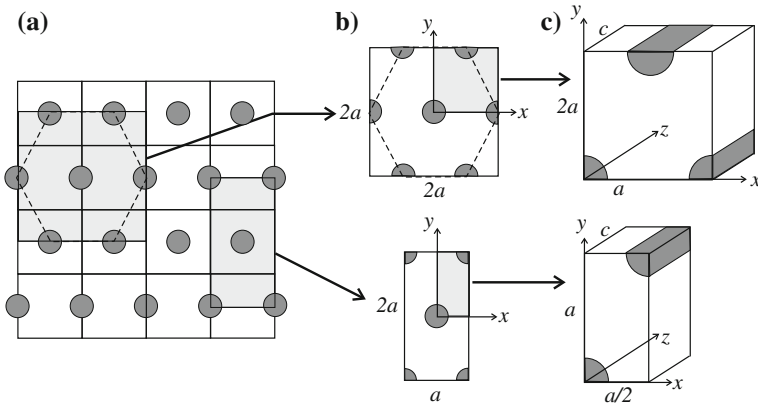
Fig. 3.8 Representative Unit Cells RUCs of hexagonal symmetry: **a** various choices of repeating RUCs at the macrolevel, **b** two different geometries of repeating RUCs—square and rectangular and corresponding fibers configuration, **c** shape and fibers disposition in two sub-RUCs with additional symmetry used

(Fig. 3.7b) have 4 axes of geometrical symmetry whereas the *RUCs of the hexagonal symmetry* (Fig. 3.8b) inscribed into the $2a \times 2a$ square or the $a \times 2a$ rectangle have only 2 axes of geometrical symmetry, in spite of that the hexagonal has 6 own symmetry axes. A choice of subcells (Fig. 3.7c and Fig. 3.8c) used for homogenization is in fact arbitrary and does not influence final numerical results, but proper distinction between the tetragonal and the hexagonal RUCs (Fig. 3.7 vs. Fig. 3.8) should follow the *true fibers arrangement* during composite fabrication in order to properly estimate mechanical characteristics of the composite which meet the experimental findings (see Sect. 3.5.3).

3.5.3 Sun and Vaidya Findings for Boron/Al Composite

In what follows let us inspect some results presented in Sun and Vaidya [30] for *transversely isotropic Boron/Aluminum composite* by the use of *FEM micromechanics-based homogenization* models when compared to other methods, c.f. Hashin and Rosen [10], Chamis [6] for various fibers topology (square array vs. hexagonal array) and some experimental evidence. The isotropic material properties of both constituents: *Boron fiber* and *Aluminum matrix* used by the authors are recalled in Table 3.4.

Key to distinct elastic response of the transversely isotropic (unidirectional) composite of either the *tetragonal* or the *hexagonal symmetry* is a number of independent material constants. In general case of the composite that exhibits plane isotropy property of tetragonal type, the averaged composite material is characterized by six

Table 3.4 Material properties of isotropic constituents of the unidirectional Boron fibers reinforcement in the Aluminum matrix, after Sun and Vaidya [30]

Constituent material	E (GPa)	ν
Boron fiber	379.3	0.1
Aluminum matrix	68.3	0.3

independent constants: E_{11}, E_{33}, ν_{21}, ν_{32}, G_{23}, and G_{12}. By contrast, in case of plane isotropy of hexagonal type the number of independent material constants is reduced to five since the shear modulus in the isotropy plane G_{23} is coupled with the transverse Young modulus E_{22} and corresponding Poisson ratio ν_{23} by the relationship which holds for isotropic media

$$G_{23} = \frac{E_{22}}{2(1 + \nu_{23})} \tag{3.60}$$

Let us examine the data given in Table 3.5 based on Sun and Vaidya [30] in the light of above constraint. It is visible that in case of micromechanics-based FEM model with the hexagonal array used by Sun and Vaidya [30] as well as its simulations by Hashin and Rosen [10] the *transversely isotropic hexagonal symmetry* roughly holds Eq. (3.60). However, when the RUC of *tetragonal symmetry* (square array) is used by Sun and Vaidya [30] or Chamis [6] composite exhibits the tetragonal symmetry property.

Note also that in literature a big scatter of both the material properties of the constituents of the same type (Boron/Al) and results based on different homogenization methods are met.

Table 3.5 Comparison of selected elastic material modules for the Boron/Al composite, obtained in various numerical experiments by different authors for the same Boron/Al composite material ($V_f = 0.47$), after Sun and Vaidya [30]

Material constants of composite Boron/Al ($V_f = 0.47$)	FEM Sun and Vaidya [30]		Numerical simulations	
	Square array	Hexagonal array	Chamis [6]	Hashin and Rosen [10]
E_{11} (GPa)	215	215	214	215
$E_{22} = E_{33}$ (GPa)	144	136.5	156	139.1
G_{23} (GPa)	45.9	52.5	43.6	54.6
$G_{12} = G_{13}$ (GPa)	57.2	54.0	62.6	53.9
ν_{32}	0.29	0.34	0.31	0.31
$\nu_{21} = \nu_{31}$	0.19	0.19	0.20	0.195

3.5.4 Interpretation of the Theorem of Lower and Upper Bounds in the Light of Gan et al. [9] and Aboudi et al. [1] Findings for Boron/Al Composite

Sun and Vaidya findings presented in Sect. 3.5.3 are limited to the selected volume fraction ($V_f = 0.47$). For further analysis it is convenient to discuss Gan et al. [9] findings concerning the similar Boron/Al long-fiber composite Table 3.6, but obtained for a complete volume fraction spectrum $V_f \in [0, 1]$.

Note large discrepancy between the input data used for numerical experiments by Sun and Vaidya [30] (Table 3.4) and that used by Gan et al. [9] (Table 3.6). In numerical experiments based on homogenization methods FEM, GMC and SCMS (see Sect. 3.5.1) Gan et al. [9] compared various round Boron fiber arrangements in the RUC: *unidirectional random* (disordered) *disposition*, the *single fiber* centered *in the square cell* and the *hexagonal symmetry array*, but applying the *general orthotropy symmetry group* (9 material constants explored), see Fig. 3.1. Results obtained from numerical experiments FEM, GMC and SCMC (Table 3.7) closely resemble data governed by the transverse symmetry group, but in case of GMC method a higher divergence is met. Further distinction between the tetragonal or the hexagonal symmetry group can be done by checking the condition (3.60). An analysis performed in Table 3.8 leads to the conclusion that the considered composite exhibits the *tetragonal symmetry class* when *GMC* and *SCMC homogenization methods* are involved since the condition (3.60) does not hold. By contrast, when the *micromechanics-based FEM* was implemented the results obtained satisfy the requirement of the *hexagonal symmetry class* (condition (3.60) is satisfied) where only 5 material constants are essentially independent (see Fig. 3.1 and Eq. 3.13 vs. 3.14).

Examine closer the selected Gan et al. [9] findings from numerical experiments based on the regular hexagonal fibers packing in the Boron/Al composite by the use of SCMC homogenization method, compared with the Voigt and Reuss models relied upon the volume fractions of the phases only. Inspection of these results obtained in numerical experiment for long-fiber-reinforced composite characterized by *transversely isotropic tetragonal* or *hexagonal symmetry* performed in light of the *Hill theorem on lower and upper bounds by Voigt* and *Reuss isotropic estimates* will be subject of further considerations.

Chronologically, Voigt (1889) and Reuss (1929) had proposed estimates for engineering constants E and G in polycrystals a long time before Hill proved famous theorem on lower and upper bounds for the *averaged stiffness matrix* $[\overline{\mathbb{E}}]$ or the *com-*

Table 3.6 Material properties of constituents of the unidirectional Boron/Al composite, after Gan et al. [9]

Constituent material	E (GPa)	ν
Boron fiber	413.7	0.2
Aluminum matrix	55.16	0.3

Table 3.7 Approximation of material constants by orthotropic numerical experiment for unidirectional long-fiber Boron/Al composite with random fibers arrangement in-plane transverse to fibers beam direction and 30×30 number od subcells in the RVE, after Gan et al. [9]

Material constants of Boron composite/Al ($V_f = 0.5$)	Homogenization methods (random arrangement of fibers)		
	FEM	GMC	SCMC
E_{11} (GPa)	234.7	234.7	234.7
E_{22} (GPa)	138.5	117.9	131.0
E_{33} (GPa)	137.3	113.1	128.6
G_{23} (GPa)	54.78	37.78	57.70
G_{21} (GPa)	60.48	42.94	58.51
G_{31} (GPa)	60.99	40.53	58.77
ν_{21}	0.2361	0.2446	0.2387
ν_{31}	0.2369	0.2492	0.2405
ν_{32}	0.3078	0.3289	0.3182

Table 3.8 Comparison of the shear modules in the transverse plane obtained from the experiment by Gan et al. [9] for random unidirectional fibers dispersion in RVE (orthotropy) of Boron/Al composite with the expected magnitude under the hexagonal-type transverse isotropy constraint (3.60)

	FEM	GMC	SCMC
G_{23} (GPa)	54.78	37.78	57.70
$G_{23} = \frac{E_{22}}{2(1+\nu_{32})}$	52.7	43.45	49.23
% of divergence	-3.9	13.0	-17.2

pliance matrix $[\overline{\mathbb{E}}^{-1}]$ addressed to heterogeneous media (see Hill [13]). Recently, scientists involved in the composite mechanics field and development of reliable homogenization methods, commonly employ the Hill theorem originated for multiphase media, to estimate numerically the effective stiffness or compliance matrices for composite materials. Very often they need to find the engineering constants which are conventional input data for existing FEM-based codes addressed to anisotropic composites. As a consequence, magnitudes of the Young modules E_{11}, E_{22}, E_{33} and the Kirchhoff modules G_{12}, G_{23}, G_{31} counted from $[\overline{\mathbb{E}}]$ or $[\overline{\mathbb{E}}^{-1}]$ lay inside the Voigt and the Reuss estimates. Contrary, the magnitudes of Poisson ratios ν_{12}, ν_{23}, ν_{31}, that may exceed both estimates, even though the Hill theorem on lower and upper bounds holds for all elements of averaged stiffness $[\overline{\mathbb{E}}]$ or compliance $[\overline{\mathbb{E}}^{-1}]$ matrices. Such peculiarity occurs although the theorem on Voigt and Reuss estimates is fulfilled, if consistently applied to all elements of elastic matrices $[\overline{\mathbb{E}}]$ or $[\overline{\mathbb{E}}^{-1}]$, but not to the engineering constants evaluated from the appropriate formulas. Note that the engineering constants are measured from experiments. Such peculiarity can be observed

for instance in results for the *Boron/Al composites* presented by Gan et al. [9] Fig. 3.9, as well as the another *Glass/Epoxy composites* by Aboudi et al. [1], see Fig. 3.10.

Presented in the Fig. 3.9 *Voigt* and *Reuss' bounds* are obtained in two different ways. First, the *"loose" bounds* are obtained by extracting the averaged Poisson ratios from the appropriate stiffness matrix element, which will be discussed further. Second, the *"tight" bounds* are obtained in the way of straightforward use of Voigt and Reuss' mixture rules to Poisson ratios of both phases. It is evident that the exemplary results by Gan et al. [9] obtained by application of SCMC method exceed both "loose" as well as "tight" systems of bounds. Similar behavior is typical also for another *Glass/Epoxy composite* system discussed by Aboudi et al. [1], see Fig. 3.10. The Voigt and the Reuss bounds used here are enriched by other "loose" bounds of *Concentric Cylindrical Assemblage model* (CCA$^+$, CCA$^-$) which turn out to be much broader. Although such a broad bound systems are admitted, the Poisson ratios

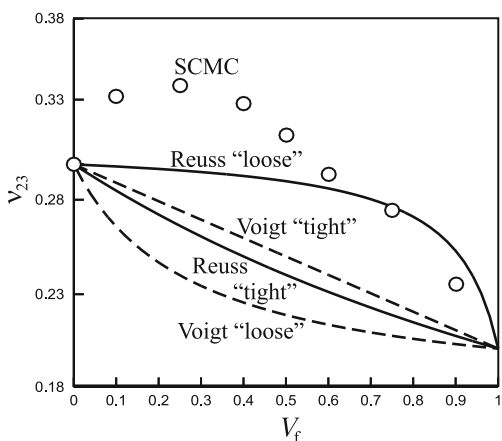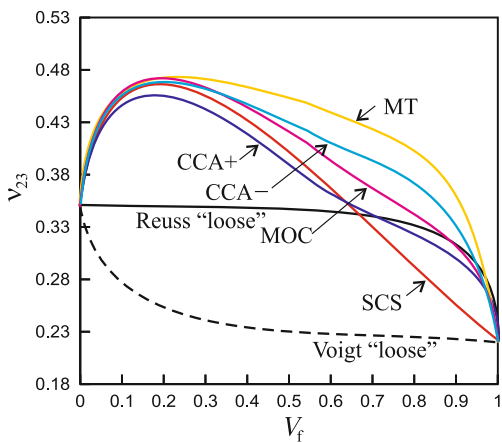**Fig. 3.9** Peculiarity of the Poisson ratio ν_{23} diagrams for the long-fiber *Boron/Al system*, after Gan et al. [9]

Fig. 3.10 Peculiarity of the Poisson ratio ν_{23} diagrams for the long-fiber *Glass/Epoxy composite*, system after Aboudi et al. [1]

ν_{23} obtained by use of the *Mori–Tanaka method* (MT), the *Micromechanics-based Method of Cells* (MMC) and the *Self Consistent Scheme* (SCS) exceed these bounds.

Note that in both cases the "loose" Voigt and Reuss bounds are shown by two curved diagrams versus V_f in Figs. 3.9 and 3.10, although the Voigt estimate is in fact linear (from definition). It can be understood when the mixture rules, Voigt and Reuss', are consistently applied to the *stiffness modulus of* $E_{11}^{r/m}$ both *phases*, matrix and fiber reinforcement

$$E_{11}^{m/r} \overset{\text{def}}{=} \frac{E^{m/r}(1 - \nu^{m/r})}{(1 + \nu^{m/r})(1 - 2\nu^{m/r})} \tag{3.61}$$

namely

$$^V\overline{E}_{11} = E_{11}^m(1 - V_r) + E_{11}^r V_r$$
$$\frac{1}{^R\overline{E}_{11}} = \frac{(1 - V_r)}{E_{11}^m} + \frac{V_r}{E_{11}^r} \tag{3.62}$$

Bars in Eq. (3.62) over the symbol refer to the composite as a whole, superscripts ^{V} and ^{R} refer to the *Voigt* and *Reuss' estimates* whereas symbols $^{m/r}$ refer to the constituents (matrix and fiber reinforcement). Symbols $^{V/R}\overline{E}_{11}$ are given by the following formulas

$$^V\overline{E}_{11} = \frac{^V\overline{E}(1 - {}^V\overline{\nu})}{(1 + {}^V\overline{\nu})(1 - 2\,{}^V\overline{\nu})}$$
$$^R\overline{E}_{11} = \frac{^R\overline{E}(1 - {}^R\overline{\nu})}{(1 + {}^R\overline{\nu})(1 - 2\,{}^R\overline{\nu})} \tag{3.63}$$

Solution of the above equation system (3.63) for the magnitudes of averaged *Poisson ratio* $\overline{\nu}$ with the *Young modules* $^V\overline{E}$, $^R\overline{E}$ *averaged* straightforwardly *by* the use of appropriate *mixture rules* for Voigt and Reuss' estimates

$$^V\overline{E}(V_f) = E^m(1 - V_f) + E^r V_f$$
$$\frac{1}{^R\overline{E}(V_f)} = \frac{1 - V_f}{E^m} + \frac{V_f}{E^r} \tag{3.64}$$

yields the following formula for the "loose" Poisson ratio bounds

$$^{V/R}\overline{\nu} = \frac{\sqrt{\left(1 - \frac{^{V/R}\overline{E}_{11}}{^{V/R}\overline{E}}\right)^2 - 8\left(1 - \frac{^{V/R}\overline{E}_{11}}{^{V/R}\overline{E}}\right)\frac{^{V/R}\overline{E}_{11}}{^{V/R}\overline{E}} + 1} - \frac{^{V/R}\overline{E}_{11}}{^{V/R}\overline{E}}}{4\frac{^{V/R}\overline{E}_{11}}{^{V/R}\overline{E}}} \tag{3.65}$$

Alternatively, applying the Voigt or the Reuss mixture rules directly to the Poisson ratios of both phases, matrix ν^m and fiber ν^r other two "tight" Poisson ratio bounds are found

$$^\text{V}\overline{\nu} = \nu^\text{m}(1 - V_\text{f}) + \nu^\text{r}V_\text{f}$$
$$\frac{1}{^\text{R}\overline{\nu}} = \frac{1 - V_\text{f}}{\nu^\text{m}} + \frac{V_\text{f}}{\nu^\text{r}}$$

(3.66)

where the "tight" Voigt bound preserves linearity.

Concluding, both "loose" bounding diagrams in Figs. 3.9 and 3.10 exhibit non-linear property since the magnitudes of Poisson ratios were obtained in an artificial paths: either by extracting them from Eq. (3.63) or by straightforward application of the mixture rules to engineering Poisson ratios for which linear "tight" Voigt estimate is saved (3.66).

Finally, when the *Hill theorem of lower and upper bounds* is consistently applied to the elements of *elastic stiffness* or *compliance matrices* then and only then all *effective matrix elements of* a *composite* considered lay inside the lower and upper bounds or at most at one of the bounds. In fact, if the results by Gan et al. [9], originally presented in terms of the *engineering anisotropic constants* $E_{11}, E_{22}, G_{23}, G_{12}, \nu_{12}$ and ν_{23} are consistently transformed to the space of elements of compliance matrix $\overline{E}_{11}^{-1}, \overline{E}_{33}^{-1}, \overline{E}_{12}^{-1}, \overline{E}_{23}^{-1}, \overline{E}_{44}^{-1}, \overline{E}_{55}^{-1}$, the results obtained by use of the SCMC method follow the Hill theorem upper and lower bounds as shown in Fig. 3.11.

3.5.5 Approximation of Mechanical Modules of Long-Fiber Unidirectionally Reinforced Composites by the Use of a Hybrid Rule Between Voigt and Reuss Estimates

Mention at the beginning that classical mixture rules by Voigt (3.17_1) and Reuss (3.17_2) apply a random dispersion of composite constituents over RVE. It is obvious that the Voigt and the Reuss estimates converge at appropriate magnitudes of modules of matrix and reinforcement for *volume fraction* $V_\text{f} = 0$ or $V_\text{f} = 1$, respectively. This question should be carefully considered in light of fabrication procedure. Namely, assuming identical fibers of circular cross-section regularly packed over the RUC either according to square or hexagonal arrays we arrive at two different *maximal fiber packing limits* V_fmax, see Fig. 3.12. It is seen that maximal fiber packing for the *square array* $V_\text{fmax}^\text{sq} \cong 78.5\,\%$ is much lower than analogous maximal fiber packing for the *hexagonal array* $V_\text{fmax}^\text{hex} \cong 90.7\,\%$. Even higher maximal fiber packing can be achieved by using fibers of either various diameters or noncircular cross-section (*square* cross-section *fibers* or *honey-comb* cross-section *fibers* joined by thin matrix layers). Hence, the homogenization results according to Voigt or Reuss for surroundings $V_\text{f} \cong 1$ have only theoretical sense. Analogous objections can be formulated to homogenization results for surroundings $V_\text{f} \cong 0$ where there is difficult to talk about a composite.

Consider now in detail results by Gan et al. [9]. In what follows in order to formulate a *weighted homogenization rule* based on a tensorial interpolation between lower and upper bounds it will be more convenient to consistently formulate the Voigt and Reuss estimates in application to stiffness or compliance matrix components but
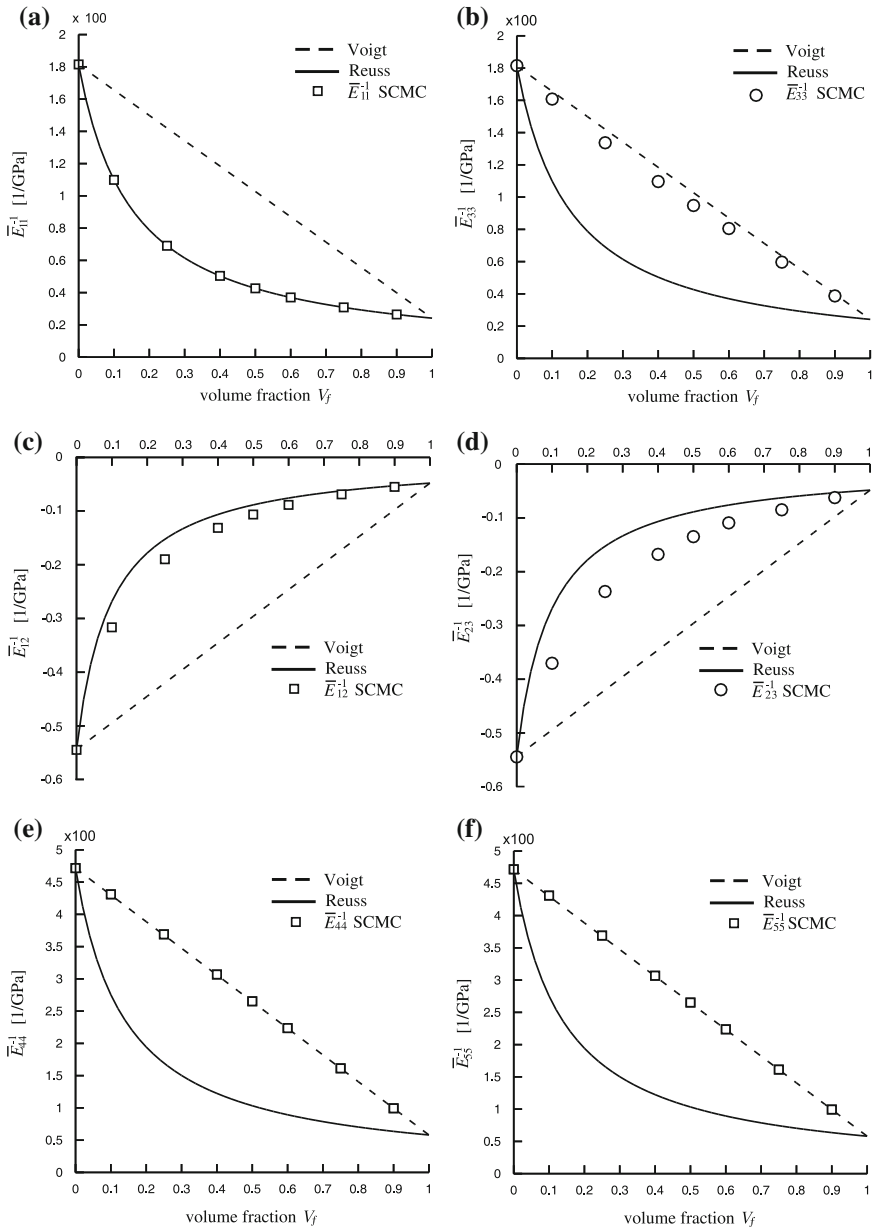
Fig. 3.11 Interpretation of the Gan et al. [9] results in the space of elements of effective compliance matrix $[\overline{\mathbb{E}}^{-1}]$ obtained on the base of diagrams of engineering constants of the Boron/Al composite in light of theorem of upper and lower bounds by the Voigt and Reuss estimates
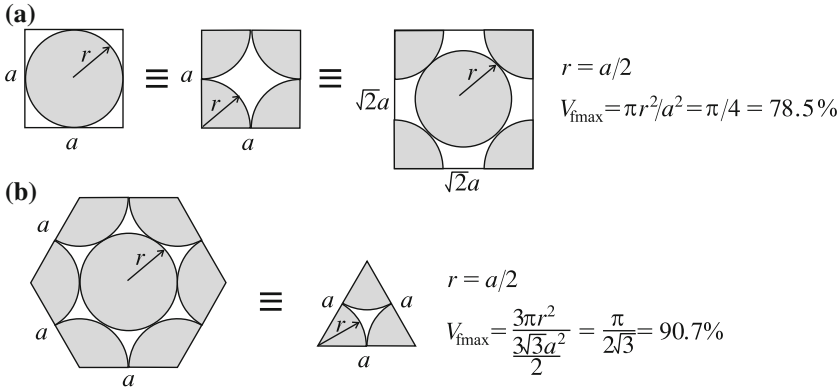
(a)

(b)

Fig. 3.12 Illustration of maximal fiber packing for identical fibers of circular cross-section in case of: **a** square array, **b** hexagonal array

not to the engineering constants (what is commonly done). The weighted homogenization rule allows to formulate the approximate method to estimate elements of effective elasticity matrices (stiffness or compliance) by the use of the values of lower and upper bounds and performing interpolation between them with the use of new *tensor-like rule of mixture* (a *hybrid formulation*). In this way it will be possible to build diagrams for all *orthotropic matrix components* $[\mathbb{E}^{-1}]$ in the full range of volume fraction $V_f \in [0, 1]$ assuming coincidence with known experimentally obtained matrix $[^{exp}\mathbb{E}^{-1}]$ for one arbitrarily chosen volume fraction V_f^0. Additionally, coincidence with known matrices of pure constituents: $V_f = 0$ for matrix material and $V_f = 1$ for fiber material must hold.

Let us rewrite the scalar Voigt and Reuss formulas (3.17) into matrix Voigt and Reuss formulas, respectively to stiffness or compliance matrices

$$^V[\overline{\mathbb{E}}] = c_1[^r\mathbb{E}] + c_2[^m\mathbb{E}] \tag{3.67}$$

or

$$^R[\overline{\mathbb{E}}^{-1}] = c_1[^r\mathbb{E}^{-1}] + c_2[^m\mathbb{E}^{-1}] \tag{3.68}$$

where common fractional concentrations by volume of the phases according Voigt and Reuss' rules $c_1 = V_f$ and $c_2 = 1 - V_f$ as previously shown for uniaxial models (3.24), see Aboudi et al. [1]. This simplification means that orientation of reinforcement is ignored, such that fractional concentrations depend on volume fraction V_f only. Symbols $[^{r/m}\mathbb{E}]$ and $[^{r/m}\mathbb{E}^{-1}]$ stand for elements of stiffness or compliance matrices for reinforcing fiber or matrix, respectively. As a matter of fact c_1 and c_2 must account for both volume fraction and reinforcement orientation, therefore for determination of them advanced homogenization schemes are required (e.g., FEM, GMC, SCMC, CCM and others).

In what follows a simple rule of *weighted average between*, the Voigt and the Reuss *upper and lower estimates* is proposed. Such approach is based on *tensorial interpolation between upper and lower estimates* which enables to avoid application of numerous cumbersome homogenization methods, for instance micromechanics-based FEM, GMC, SCMC, CCM etc.

To this end, we define weighting vector α_k built of weighting coefficients for subsequent elements of stiffness or compliance matrices. For brevity we confine ourselves to the compliance matrix only. Hence, the proposed *hybrid* or *weighting homogenization rule* takes the following format

$$\overline{\overline{E}}_{11}^{-1}(V_f) = \alpha_1^V \overline{E}_{11}^{-1}(V_f) + (1 - \alpha_1)^R \overline{E}_{11}^{-1}(V_f)$$

$$\overline{\overline{E}}_{22}^{-1}(V_f) = \alpha_2^V \overline{E}_{22}^{-1}(V_f) + (1 - \alpha_2)^R \overline{E}_{22}^{-1}(V_f)$$

$$\overline{\overline{E}}_{33}^{-1}(V_f) = \alpha_3^V \overline{E}_{33}^{-1}(V_f) + (1 - \alpha_3)^R \overline{E}_{33}^{-1}(V_f)$$

$$\overline{\overline{E}}_{23}^{-1}(V_f) = \alpha_4^V \overline{E}_{23}^{-1}(V_f) + (1 - \alpha_4)^R \overline{E}_{23}^{-1}(V_f)$$

$$\overline{\overline{E}}_{13}^{-1}(V_f) = \alpha_5^V \overline{E}_{13}^{-1}(V_f) + (1 - \alpha_5)^R \overline{E}_{13}^{-1}(V_f) \qquad (3.69)$$

$$\overline{\overline{E}}_{12}^{-1}(V_f) = \alpha_6^V \overline{E}_{12}^{-1}(V_f) + (1 - \alpha_6)^R \overline{E}_{12}^{-1}(V_f)$$

$$\overline{\overline{E}}_{44}^{-1}(V_f) = \alpha_7^V \overline{E}_{44}^{-1}(V_f) + (1 - \alpha_7)^R \overline{E}_{44}^{-1}(V_f)$$

$$\overline{\overline{E}}_{55}^{-1}(V_f) = \alpha_8^V \overline{E}_{55}^{-1}(V_f) + (1 - \alpha_8)^R \overline{E}_{55}^{-1}(V_f)$$

$$\overline{\overline{E}}_{66}^{-1}(V_f) = \alpha_9^V \overline{E}_{66}^{-1}(V_f) + (1 - \alpha_9)^R \overline{E}_{66}^{-1}(V_f)$$

Additionally, independence of the weighting coefficients α_k of the volume fraction V_f over the whole range of $V_f \in [0, 1]$ is assumed. This assumption refers to definition of convex set of two vectors. If the magnitudes of stiffness or compliance elements are known at certain point $V_f = V_f^0$

$$[\overline{\overline{\mathbb{E}}}^{-1}(V_f^0)] = [^{\exp}\mathbb{E}^{-1}(V_f^0)] \qquad (3.70)$$

then it is possible to determine unknown *vector of weighting coefficients* α_k for the compliance. Applying these coefficients over the whole range of volume fraction $V_f \in [0, 1]$ the sought elements of compliance matrix can be determined.

3.5.6 Capability of the Proposed Hybrid-Type Rule Versus Experimental Evidence in Light of Fiber Array Symmetry: Tetragonal or Hexagonal

The *weighting average homogenization rules* defined in the previous Sect. 3.5.5 by Eqs. (3.69) are rather simple and effective ones that allow to easily predict unknown

Table 3.9 Values of weight coefficients according to compliance matrix components for Voigt and Reuss' homogenization and SCMC [9]

$[\mathbb{E}^{-1}]$	Interpolation points			α_k
	$[^{\mathrm{V}}\mathbb{E}^{-1}] \times 10^{-2}$ (GPa^{-1})	$[^{\mathrm{R}}\mathbb{E}^{-1}] \times 10^{-2}$ (GPa^{-1})	$[^{\mathrm{SCMC}}\mathbb{E}^{-1}] \times 10^{-2}$ (GPa^{-1})	
E_{11}^{-1}	1.01	0.42	0.909	0.833
E_{22}^{-1}	1.01	0.42	0.909	0.833
E_{33}^{-1}	1.01	0.42	0.463	0.075
E_{23}^{-1}	−0.29	−0.09	−0.116	0.142
E_{13}^{-1}	−0.29	−0.09	−0.116	0.142
E_{12}^{-1}	−0.29	−0.09	−0.300	1.050
E_{44}^{-1}	2.59	1.01	2.130	0.707
E_{55}^{-1}	2.59	1.01	2.268	0.794
E_{66}^{-1}	2.59	1.01	2.130	0.707

constitutive modules of the composite system over the whole range of the volume fraction $V_{\mathrm{f}} \in [0, 1]$ providing that they are known for one V_{f}^0. Efficiency of this method is tested by the use of the results of numerical simulation by *SCMS homogenization method* [9]. To this end nine weighting coefficients α_k for the *orthotropic Boron/Al composite* are calculated by interpolation between Voigt and Reuss' estimates shown in Fig. 3.13. Magnitudes of the weighting coefficients α_k are established at the point $V_{\mathrm{f}}^0 = 0.513$ by comparison with the homogenization results SCMC by Gan et al. [9]. Obviously the weighting homogenization rule must give correct results at the end points $V_{\mathrm{f}} = 0$ and $V_{\mathrm{f}} = 1$. Calculated weighting coefficients and set of predictions $^{\mathrm{V}}\mathbb{E}^{-1}$, $^{\mathrm{R}}\mathbb{E}^{-1}$, $^{\mathrm{SCMC}}\mathbb{E}^{-1}$ for nine elements of compliance matrix are presented in Table 3.9. The results of the weighting homogenization rule are verified with the results given by Gan et al. [9] based on SCMC method, that fully confirm the assumption that weighting coefficients α_k can be treated as universal ones for the composite tested over the full range of volume fraction as shown by curves of weight rule ● versus SCMC homogenization □.

3.5.7 Interpretation of Results Obtained by Weighting Homogenization in Terms of Engineering Constants

Nevertheless the formulated in previous subsection *"hybrid" mixture rules* based on *weighting interpolation* between Voigt and Reuss' estimates have to be formulated in the space of elements of elasticity matrix (compliance or stiffness), where Hill theorem of lower and upper estimates by Voigt and Reuss holds, it is usually necessary to express the results in terms of *engineering orthotropy constants*. The reason for such representation results from usually applied homogenization techniques to engineering constants, but not to elasticity elements. This system of engineering
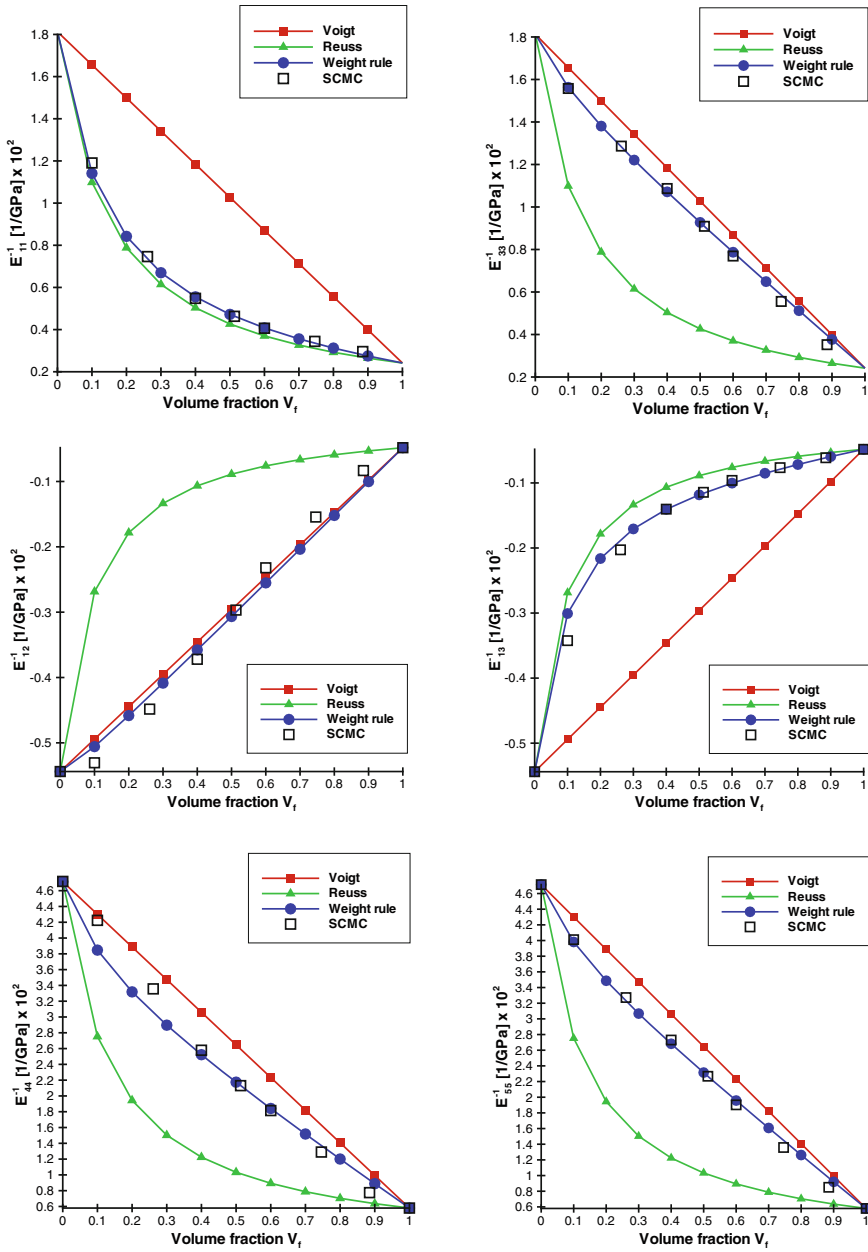
Fig. 3.13 Comparison of SCMC [9], Voigt, Reuss and proposed hybrid rule according to compliance matrix coefficients

constants is dominant in the subject literature, see Aboudi et al. [1], Gan et al. [9], Sun and Vaidya [30], and others.

To this end the engineering constants have to be extracted either from the compliance

$$
\begin{array}{lll}
E_{11} = 1/\overline{\overline{E}}_{11}^{-1} & E_{22} = 1/\overline{\overline{E}}_{22}^{-1} & E_{33} = 1/\overline{\overline{E}}_{11}^{-1} \\
G_{44} = 1/\overline{\overline{E}}_{44}^{-1} & G_{55} = 1/\overline{\overline{E}}_{55}^{-1} & G_{66} = 1/\overline{\overline{E}}_{66}^{-1} \\
\nu_{12} = -\overline{\overline{E}}_{12}^{-1}/\overline{\overline{E}}_{11}^{-1} & \nu_{13} = -\overline{\overline{E}}_{13}^{-1}/\overline{\overline{E}}_{11}^{-1} & \nu_{23} = -\overline{\overline{E}}_{23}^{-1}/\overline{\overline{E}}_{22}^{-1}
\end{array} \tag{3.71}
$$

or the stiffness

$$
\begin{aligned}
E_{11} &= \frac{2\overline{\overline{E}}_{12}\overline{\overline{E}}_{13}\overline{\overline{E}}_{23} + \overline{\overline{E}}_{11}\overline{\overline{E}}_{22}\overline{\overline{E}}_{33} - \overline{\overline{E}}_{33}\overline{\overline{E}}_{12}^2 - \overline{\overline{E}}_{11}\overline{\overline{E}}_{23}^2 - \overline{\overline{E}}_{22}\overline{\overline{E}}_{13}^2}{\overline{\overline{E}}_{22}\overline{\overline{E}}_{33} - \overline{\overline{E}}_{23}^2} \\
E_{22} &= \frac{2\overline{\overline{E}}_{12}\overline{\overline{E}}_{13}\overline{\overline{E}}_{23} + \overline{\overline{E}}_{11}\overline{\overline{E}}_{22}\overline{\overline{E}}_{33} - \overline{\overline{E}}_{33}\overline{\overline{E}}_{12}^2 - \overline{\overline{E}}_{11}\overline{\overline{E}}_{23}^2 - \overline{\overline{E}}_{22}\overline{\overline{E}}_{13}^2}{\overline{\overline{E}}_{11}\overline{\overline{E}}_{33} - \overline{\overline{E}}_{13}^2} \\
E_{33} &= \frac{2\overline{\overline{E}}_{12}\overline{\overline{E}}_{13}\overline{\overline{E}}_{23} + \overline{\overline{E}}_{11}\overline{\overline{E}}_{22}\overline{\overline{E}}_{33} - \overline{\overline{E}}_{33}\overline{\overline{E}}_{12}^2 - \overline{\overline{E}}_{11}\overline{\overline{E}}_{23}^2 - \overline{\overline{E}}_{22}\overline{\overline{E}}_{13}^2}{\overline{\overline{E}}_{11}\overline{\overline{E}}_{22} - \overline{\overline{E}}_{12}^2} \\
G_{44} &= \overline{\overline{E}}_{44} \qquad G_{55} = \overline{\overline{E}}_{55} \qquad G_{66} = \overline{\overline{E}}_{66} \\
\nu_{12} &= \frac{\overline{\overline{E}}_{12}\overline{\overline{E}}_{33} - \overline{\overline{E}}_{13}\overline{\overline{E}}_{23}}{\overline{\overline{E}}_{22}\overline{\overline{E}}_{33} - \overline{\overline{E}}_{23}^2} \qquad \nu_{13} = \frac{\overline{\overline{E}}_{13}\overline{\overline{E}}_{22} - \overline{\overline{E}}_{12}\overline{\overline{E}}_{23}}{\overline{\overline{E}}_{22}\overline{\overline{E}}_{33} - \overline{\overline{E}}_{23}^2} \\
\nu_{23} &= \frac{\overline{\overline{E}}_{23}\overline{\overline{E}}_{11} - \overline{\overline{E}}_{13}\overline{\overline{E}}_{12}}{\overline{\overline{E}}_{11}\overline{\overline{E}}_{33} - \overline{\overline{E}}_{13}^2}
\end{aligned} \tag{3.72}
$$

matrices.

In what follows the conversion of results shown in the previous section given in the elasticity modules space, to the system of engineering orthotropic constants is done preserving previously used assumption of the *transversely isotropic hexagonal symmetry*. The comparison of engineering orthotropic constants is presented in Fig. 3.14. The figure contains only four plots, because the transversely isotropic hexagonal symmetry assumption has been proven and Poisson's ratios are not discussed. Young and Kirchhoff modules obtained from proposed weighting rule (3.69) coincide with the Gan et al. [9] results.
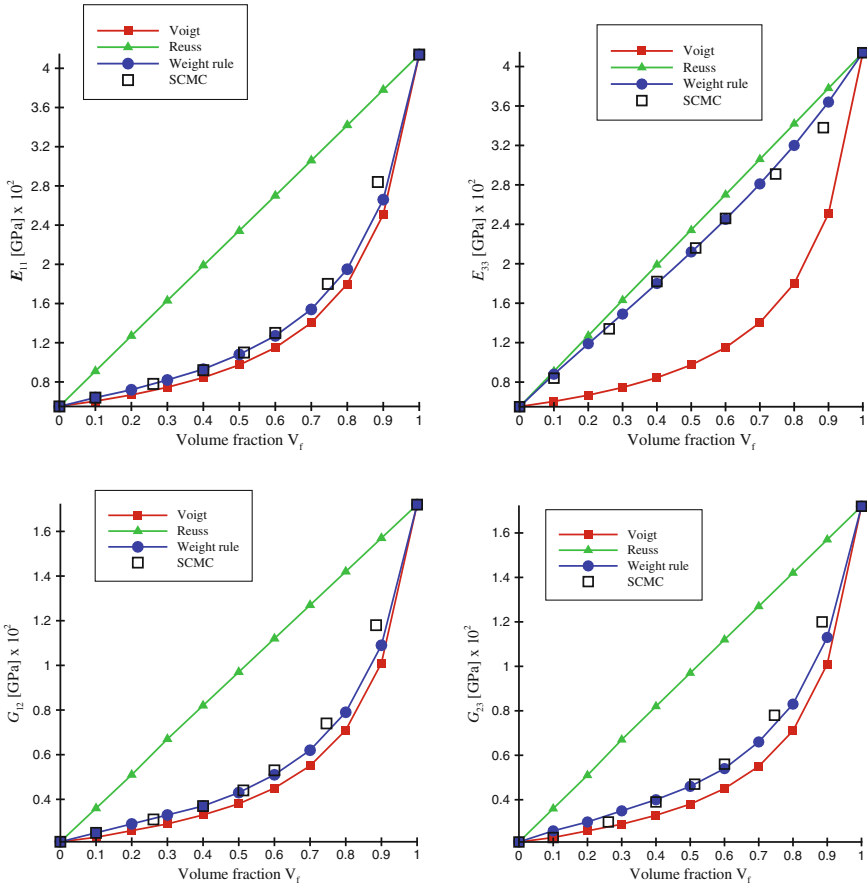
Fig. 3.14 Comparison of SCMC [9], Voigt, Reuss' and proposed hybrid estimates in the engineering orthotropic constants domain

References

1. Aboudi, J., Arnold, S.M., Bednarcyk, B.A.: Micromechanics of Composite Materials. Elsevier, Amsterdam (2013)
2. Auriault, J.-L., Boutin, C., Geindreau, C.: Homogenization of Coupled Phenomena in Heterogenous Media, pp. 39–44. Wiley-ISTE, New York (2009)
3. Banks-Sills, L., Leiderman, V., Fang, D.: On the effect of particle shape and orientation on elastic properties of metal matrix composites. Compos. Part B **28B**, 465–481 (1997)
4. Bayat, M., Aghdam, M.M.: A micromechanics-based analysis of effects of square and hexagonal fiber arrays in fibrous composites using DQEM. Eur. J. Mech.—A/Solids **32**, 32–40 (2012)
5. Berryman, J.G.: Bounds and self-consistent estimates for elastic constants of random polycrystals with hexagonal, trigonal, and tetragonal symmetries. J. Mech. Phys. Solids **53**, 2141–2173 (2005)
6. Chamis, C.C.: Simplified composite micromechanics equations for hygral, thermal and mechanical properties. SAMPE Q. **15**, 14–23 (1984)

7. Desmorat, R., Marull, R.: Non-quadratic Kelvin models based plasticity criteria for anisotropic materials. Int. J. Plast. **27**, 328–351 (2011)
8. Drago, A., Pindera, M.-J.: Micro-macromechanical analysis of heterogeneous materials: macroscopically homogeneous vs periodic microstructures. Compos. Sci. Technol. **67**, 1246–1263 (2007)
9. Gan, H., Orozco, C.E., Herkovich, C.T.: A strain-compatible method for micromechanical analysis of multi-phase composites. Int. J. Solids Struct. **37**, 5097–5122 (2000)
10. Hashin, Z., Rosen, B.W.: The elastic moduli of fiber-reinforced materials. J. Appl. Mech. **31**, 223–232 (1964)
11. Herakovich, C.T.: Mechanics of Fibrous Composites. Wiley, New York (1998)
12. Herakovich, C.T., Aboudi, J.: Thermal effects in composites. In: Hetnarski, R.B. (ed.) Stresses, Thermal, pp. 1–142. Lastran Corporation-Publishing Division, Rochester (1999)
13. Hill, R.: Elastic properties of reinforced solids: some theoretical principles. J. Mech. Phys. Solids **11**, 357–372 (1963)
14. Jiang, C.P., Xu, Y.L., Chueng, Y.K., Lo, S.H.: A rigorous analytical method for doubly periodic cylindrical inclusions under longitudinal shear and its application. Mech. Mater. **36**, 225–237 (2004)
15. Kenaga, D., Doyle, J.F., Sun, C.T.: The characterization of boron/aluminium in the nonlinear ranges as an orthotropic elastic plastic material. J. Compos. Mater. **27**, 516–531 (1987)
16. Lekhnitskii, S.G.: Theory of Elasticity of an Anisotropic Body (trans: English). Mir Publishers, Moscow (1981)
17. Li, S.: Boundary conditions for unit cells from periodic microstructures and their implications. Compos. Sci. Technol. **68**, 1962–1974 (2008)
18. Li, S., Wongsto, A.: Unit cells for micromechanical analyses of particle-reinforced composites. Mech. Mater. **36**, 543–572 (2004)
19. Liu, B., Feng, X., Zhang, S.-M.: The effective Young's modulus of composites beyond the Voigt estimation due to the Poisson effect. Compos. Sci. Technol. **69**, 2198–2204 (2009)
20. Love, A.E.H.: Mathematical Theory of Elasticity. Dover Publications, New York (1944)
21. Martin-Herrero, J., Germain, C.: Microstructure reconstruction of fibrous C/C composites from X-ray microtomography. Carbon **45**, 1242–1253 (2007)
22. Mori, T., Tanaka, K.: Average stress in matrix and average elastic energy of materials with misfitting inclusions. Acta Metall. **21**, 571–574 (1973)
23. Nye, J.F.: Własności fizyczne kryształów. PWN, Warszawa (1962)
24. Ochoa, O.O., Reddy, J.N.: Finite Element Analysis of Composite Laminates. Kluwer Academic Publishers, Dordrecht (1992)
25. Paley, M., Aboudi, J.: Micromechanical analysis of composites by generalized method of cells. Mech. Mater. **14**, 127–139 (1992)
26. Pidaparti, R.M.V., May, A.W.: A micromechanical analysis to predict the cord-rubber composite properties. Compos. Struct. **34**, 361–369 (1996)
27. Reuss, A.: Berechnung der Flissgrenze von Mischkristallen auf Grund der Plastizitätsbedingung für Einkristalle. Z. angew. Math. Mech. **9**, 49–58 (1929)
28. Selvadurai, A.P.S., Nikopour, H.: Transverse elasticity of a unidirectionally reinforced composite with an irregular fiber arrangement: experiments, theory and computations. Compos. Struct. **94**, 1973–1981 (2012)
29. Sun, C.T., Chen, J.L.: A micromechanical model for plastic behavior of fibrous composites. Compos. Sci. Technol. **40**, 115–129 (1990)
30. Sun, C.T., Vaidya, R.S.: Prediction of composite properties from a representative volume element. Compos. Sci. Technol. **56**, 171–179 (1996)
31. Sun, C.T., Zhou, S.G.: Failure of quasi-isotropic composite laminates with free edges. J. Reinf. Plast. Compos. **7**, 515–557 (1988)
32. Tamma, K.K., Avila, A.F.: An integrated micro/macro modelling and computational methodology for high temperature composites. In: Hetnarski, R.B. (ed.) Thermal Stresses, pp. 143–256. Lastran Corporation-Publishing Division, Rochester (1999)

33. Tjong, S.C., Ma, Z.Y.: Microstructural and mechanical characteristics of in situ metal matrix composites. Mater. Sci. Eng. **R29**(3–4), 49–113 (2000)
34. Voigt, W.: Über die Beziehungen zwischen beiden Elastizitätskonstanten isotroper Körpär. Wied. Ann. **38**, 573–587 (1889)
35. Whitney, J.M., Riley, M.B.: Elastic properties of fiber reinforced composite materials. AIAA J. **4**, 1537–1542 (1966)
36. Wongsto, A., Li, S.: Micromechanical FE analysis of UD fibre-reinforced composites with fibers distributed at random over the transverse cross-section. Compos. Part A **36**, 1246–1266 (2005)
37. Würkner, M., Berger, H., Gabbert, U.: On numerical evaluation of effective material properties for composite structures with rhombic arrangements. Int. J. Eng. Sci. **49**, 322–332 (2011)